



Design Project Report 2

GENE 404: Interdisciplinary Design Project 2
Faculty of Engineering

Prepared for: Professor Oscar Nespoli

Prepared by:
Team 10: 3cycle
Mohamed Abayazeed (20770294)
Julia Baribeau (20792386)
Maria Fraser Semenoff (20787376)
Urban Pistek (20802700)

April 20, 2023

Contents

Table of Figures.....	iv
Table of Tables.....	v
1.0 Introduction.....	1
1.1 Project Objective.....	1
2.0 Needs Analysis.....	1
2.1 Summary of Background.....	1
2.2 Problem Reformulation.....	1
2.3 Engineering Design Specifications.....	2
2.4 Applicable Theory.....	4
3.0 Engineering Design	5
3.1 Design Overview.....	5
3.2 System Diagram.....	6
3.3 Mechanical Design	7
3.4 Hardware & Electrical Design.....	8
3.5 Software Design	10
3.5.1 Firmware Design.....	10
3.5.2 Backend Software Design.....	11
3.5.3 UX/UI Design	11
3.6 Algorithms and Machine Learning Design	12
3.6.1 Spectra Generation Algorithm	14
3.6.2 Colour Detection Algorithm	15
3.6.3 Machine Learning	16
3.7 Reformulation Summary.....	20
4.0 Engineering Verification & Validation	21
4.1 Lab Experiments.....	21
4.1.1 Spectrometry Research.....	21
4.1.2 Plastic Recycling in the Mekonnen Lab.....	23
4.1.3 Tensile Results of the Recycled Filament.....	26
4.1.4 Recycled Filament Making in the Velocity Lab	27
4.2 Design Verification	28
4.2.1 Hardware & Mechanical Verification.....	28

4.2.2 Software Verification	29
4.2.3 Machine Learning Validation.....	30
4.2.4 System Verification.....	32
5.0 Safety, Regulations and Sustainability.....	35
5.1 Design for Safety.....	35
5.2 Design for Regulatory Requirements	36
5.3 Design for Sustainability	36
5.4 Assessment of Impact of the Engineering Design on Society and the Environment	37
6.0 Project Management.....	39
6.1 Timeline & Schedule	39
6.2 Lessons Learned	40
7.0 Conclusions & Recommendations	41
7.1 Conclusions	41
7.2 Recommendations	41
7.3 Acknowledgements	42
References	44
Appendix A	46
DNIR Board Schematics: 10-2022-DNIR Rev. 1	47
Sensor.....	47
ADC.....	48
MCU.....	49
Power	50
LED	51
DNIR Board Layout	52
System Level Representation: 10-2022-SD Rev. 2	53
System Level Representation: 10-2022-SD Rev. 3	54
Engineering Design Specifications: 10-2022-EDS Rev 1, Rev 2, Rev 3, Rev 4.....	55
Code: GitHub	56
DNIR Module Parts List: 10-2022-BOM Rev 1	57
Appendix B	60
Appendix C	66
Appendix D	72

Table of Figures

Figure 1. A system diagram detailing the identification system.....	6
Figure 2. (a) Left: an enclosed cover design with collar and (b) Right: an open cover design with no collar, just standoffs to hold the sample a standard distance from the photodiode.....	7
Figure 3. Exploded view of a CAD model of the mounting arm used for the camera board.....	8
Figure 4. Hardware architecture	9
Figure 5. Firmware architecture and procedures	10
Figure 6. Backend software system diagram.....	11
Figure 7. Graphics-user interface (GUI) mock-up.....	12
Figure 8. PLA (red) vs ABS (black) reflectance readings for white, lime, and black samples.....	13
Figure 9. Calibration and noise-filtering procedure.....	15
Figure 10. Computer vision procedure for colour identification from camera input.....	16
Figure 11. Feature set generation procedure.....	17
Figure 12. PLA vs ABS vs PETG spectra to show how other plastics overlap with PLA and ABS in certain areas.....	18
Figure 13. Machine learning pipeline system diagram	19
Figure 14. Names of models trained and tested in the machine learning pipeline.	19
Figure 15. Spectrometry readings of PLA, ABS, and contaminated samples.....	22
Figure 16. Spectrometry readings of PLA and ABS of the same colour, white.	23
Figure 17. (a) Left: black PLA with grey discolouration and (b) Right: white ABS with yellowing discolouration after both underwent simulated recycling in the batchmixer.	24
Figure 18. Spectrometry of virgin PLA and twice-recycled PLA.....	25
Figure 19. Spectrometry of virgin ABS and twice-recycled ABS.....	25
Figure 20. Tensile test results of virgin and recycled PLA	26
Figure 21. Assembled apparatus with the DNIR module in its cover and the camera on its mount .	28
Figure 22. GUI Display showing camera feed, spectrum scan, inferred color, and inferred material	29
Figure 23. Model info captured during training. Includes validation accuracy, output labels, training parameters, and model hyperparameters.....	30
Figure 24. Confusion matrix of the gradient boosting classifier model for board v1.0 with the full set of trained labels: ABS, PLA, PETG, Empty, Plastics, and Non-Plastics.....	31
Figure 25. Mean square gradient boosting classifier model for board v1.0 with the full set of trained labels: ABS, PLA, PETG, Empty, Plastics, and Non-Plastics using k=100 folds.	32
Figure 26. Complete system setup, with Apparatus and DNIR module connected to a host PC running the GUI application.....	33
Figure 27. An overview of the part of SDG #12 that our project focuses on (United Nations, n.d.)....	37
Figure 28. Reduced carbon dioxide emissions from recycling 3D printer filament.....	38
Figure 29. Reduced cost of production from recycling 3D printer filament.....	39
Figure 30. The planned schedule for the project represented as coloured cells with dark shades representing planned contingency, and dashes indicating when each task was completed in the timeline. Only one task was completed after planned contingency.	40

Table of Tables

Table 1. Engineering design specifications	2
Table 2. Cost, Energy, and Emissions of Virgin Material [GrantaEdupack]	4
Table 3. Expected Mechanical Properties of Virgin ABS and PLA (Ansys, 2022)	5
Table 4. Wavelengths selected for LEDs in each version of the DNIR module.	9
Table 5. Photodiodes selected for each version of the DNIR module.	9
Table 6. Summary of selected trained models.....	20
Table 7. Mechanical property comparison of virgin and recycled PLA	26
Table 8. Verification Results of Engineering Design Specification	33
Table 9. Embodied Energy of Recycling (Ansys 2022)	37
Table 10. Speed and Energy Consumption of Felfil Machines (Felfil 2022)	37

1.0 Introduction

Refer to Design Project Report 1 (Abayazeed, Baribeau, Fraser Semenoff, & Pistek, 2022) for more details on the project background and preliminary design.

1.1 Project Objective

The big-picture goal of this project is to enable the recycling of 3D-printed waste in the Waterloo Region and beyond by identifying and filling gaps in the recycling process being established by the student startup *3cycle*.

The specific objective of this project is to reliably identify 3D-printed waste by material and colour to enable its recycling.

2.0 Needs Analysis

2.1 Summary of Background

By 2030, the use of 3D-printers is predicted to generate 7.1 million kg of plastic waste every year in the United States alone, which can be quantified by an annual landfill tipping fee of 383 million USD (Tiseo, 2022). Fused-Deposition Modelling (FDM) printers, where thermoplastic filament is melted and deposited in layers to build a 3D model, are used by hobbyists, small businesses, libraries, schools, universities, and makerspaces. Most of these small-scale users are concerned about this plastic waste (e.g., support material, rafts, failed prints, etc.) but it is not accepted by municipal recycling centres (Amri, 2022). Despite being highly recyclable, it is difficult to sort out of the waste stream. Separating the 3D-printed waste plastic by type and by colour will permit community-scale recycling, as well as ensuring a high quality of recycled filament, making the output product desirable for users and contributing to an economically sustainable recycling industry (Amri, 2022).

2.2 Problem Reformulation

The project originally aimed to create an autonomous full recycling line for 3D-printed waste, but a closer needs analysis revealed that existing solutions for shredding, extruding, and spooling recycled filament are sufficient and that the true gap existed in reliably sorting the waste to ensure a high quality in the final recycled product. Accordingly, the scope was refined to primarily focus on the reliable identification of the plastics by material.

The two most common materials used in FDM 3D-printing are polylactic acid (PLA) and acrylonitrile butadiene styrene (ABS), so the scope was narrowed to focus on their differentiation.

It was also determined that a lack of research exists surrounding the long-term consequences of recycling on 3D-printer filament and prints, so the project included laboratory experiments to predict what issues may arise with repeated recycling and how the recycling process can adapt appropriately.

2.3 Engineering Design Specifications

The specifications for design of the solution are detailed in Table 1.

Table 1. Engineering design specifications

Parameter	Relation	Value	Unit	Verification Method	Classification
Primary Specifications					
Differentiate between PLA, ABS, and “other”			Demo	Primary Function	
Reliable	within	5	%	Demo, testing	Primary Constraint
Functional Specifications					
Reject non-plastic materials	is	True/False		Demo, testing	Requirement
Sense colour	within	+/- 10	nm	Demo, testing	Requirement
Identification rate	\geq	0.15	kg/h	Demo, testing	Constraint
Accept material of appropriate size	<	9 x 10.5 x 15	cm	Demo	Constraint
Accessibility Specifications					

Cost *	within	\$4.4 (PLA) \$3.44 (ABS)	CAD/kg	Analysis	Constraint
Components available off-the-shelf or open-source			Analysis	Constraint	
Sustainability Specifications					
Energy demand*	<	47.2 (PLA) 98.3 (ABS)	MJ/kg	Analysis	Constraint
CO ₂ production*	<	2.4 (PLA) 3.77 (ABS)	kg/kg	Analysis	Constraint
Conform to <i>Restrictions on the Use of Certain Hazardous Substances (RoHS)</i> in electronic devices to prevent environmental contamination.			Analysis	Constraint	
Creates minimal by-product waste			Demo	Constraint	
Safety Specifications					
Voltage in any part of device	<	50	V	Analysis, demo, testing	Constraint
Does not contain lead, mercury, cadmium, hexavalent chromium, poly-brominated biphenyls or polybrominated diphenyl ethers except as permitted in the Annex of Directive 2002/95/EC2 for certain lead solders			Inspection	Constraint	
No exposed sharp edges or pinch points			Inspection, demo	Constraint	
Does not emit fumes			Demo	Constraint	

Conform to regulations of: International Electrotechnical Commission - (electrical device regulations) Directive 2002/95/EC - (Hazardous materials including heavy metals)	Demo	Constraint
--	------	------------

*Calculated using the data in Table 2.

Table 2. Cost, Energy, and Emissions of Virgin Material [GrantaEdupack]

Plastic Type	Cost of Production (CAD/kg)	Energy of Production (MJ/kg)	CO2 of Production (kg/kg)
PLA	3.39–4	42.6–47.2	2.16–2.4
ABS	2.14–3.13	88.9–98.3	3.41–3.77

2.4 Applicable Theory

Spectroscopy is a method of finding the molecular fingerprint of a material by measuring reflected wavelengths of light to identify molecular structures present in a material, which can then be used to identify the material type. Near-infrared (NIR) is a section of the electromagnetic spectrum, which is in the infrared range, near the visible range, and NIR spectroscopy is a method of spectroscopy which employs the NIR range of light. Discrete spectroscopy uses a few specially selected wavelengths of light to identify materials, as opposed to a continuous spectrum, which significantly reduces the complexity and cost of spectroscopy equipment.

Machine learning is a method of software design which uses labelled data to train a model to identify outputs based on a collection of inputs called a *featureset*. In this project, labelled spectra collected from plastic samples were used to train models to identify plastic types. See Section 3.6 for more details.

The reliability of 3D-prints is a key factor influencing which filament users purchase. If waste plastic is to be recycled into filament for reuse in the same application, reliability must be prioritized. One measure of reliability is the mechanical properties of the materials produced. Some common measures of strength include Young's modulus (Equation 1) and tensile strength (Equation 2) calculated using stress-strain testing. See Design Project Report 1 for more details. Table 3 summarizes mechanical properties that are expected in virgin (non-recycled) ABS and PLA.

$$E = \sigma/\varepsilon \quad (\text{Eq. 1})$$

$$\sigma_{max} = F_{max}/A_0 \quad (\text{Eq. 2})$$

Table 3. Expected Mechanical Properties of Virgin ABS and PLA (Ansys, 2022)

Mechanical Property	ABS	PLA
Young's modulus (GPA)	2.07	3.3
Tensile strength (MPA)	37.9	55
Elongation (%)	5	2.5

3.0 Engineering Design

3.1 Design Overview

The solution comprises multiple subsystems and layers of system specific components. First, an apparatus was designed to house the hardware, consisting of an enclosure that encompasses the DNIR board and an adjustable camera arm for the camera sensor.

The hardware design has not changed much since Capstone Design Report 1 other than the addition of a USB camera sensor to replace the built-in webcam for colour detection. A second DNIR board was developed mimicking the first but with a different photodiode and set of NIR LEDs.

The software stack consists of the firmware used to generate the spectra and send the data and metadata over USB serial to a compute module. A backend was developed to read the serial data from the DNIR board and the camera module, along with a processing module that takes the raw spectra data and generates the final spectra by removing different sources of noise present in the system. Finally, a Graphical User Interface (GUI) was developed to control the DNIR board and camera sensor, get the colour and sensor data, and run the machine learning model which performs the inference to determine the plastic type based on the input data.

Additionally, a set of algorithms and a machine learning pipeline and stack were developed to perform the spectra generation, colour detection and classification. A spectra generation algorithm was developed to reliably and consistently create a spectrum which removed different sources of noise in the system and captured the variance of the spectrum data. The colour detection algorithm was responsible for getting the colour of the sample which was fed into the software backend and was an input for the machine learning model. Finally, a machine learning pipeline was developed to

pre-process the data, train a model, perform validation and apply additional model optimization along with some utilities, such as data preparation and plotting.

Together these systems form the solution design. Each sub-system will be elaborated on further in the following sections.

3.2 System Diagram

The identification system is depicted with a diagram seen in Figure 1. In essence, the sample is placed on the scanner which reads its colour and NIR reflectance, noise from scattered LED light and ambient light is subtracted, the readings are compared to a labelled comprehensive database to classify the material of the sample, then the system outputs the material type and colour.

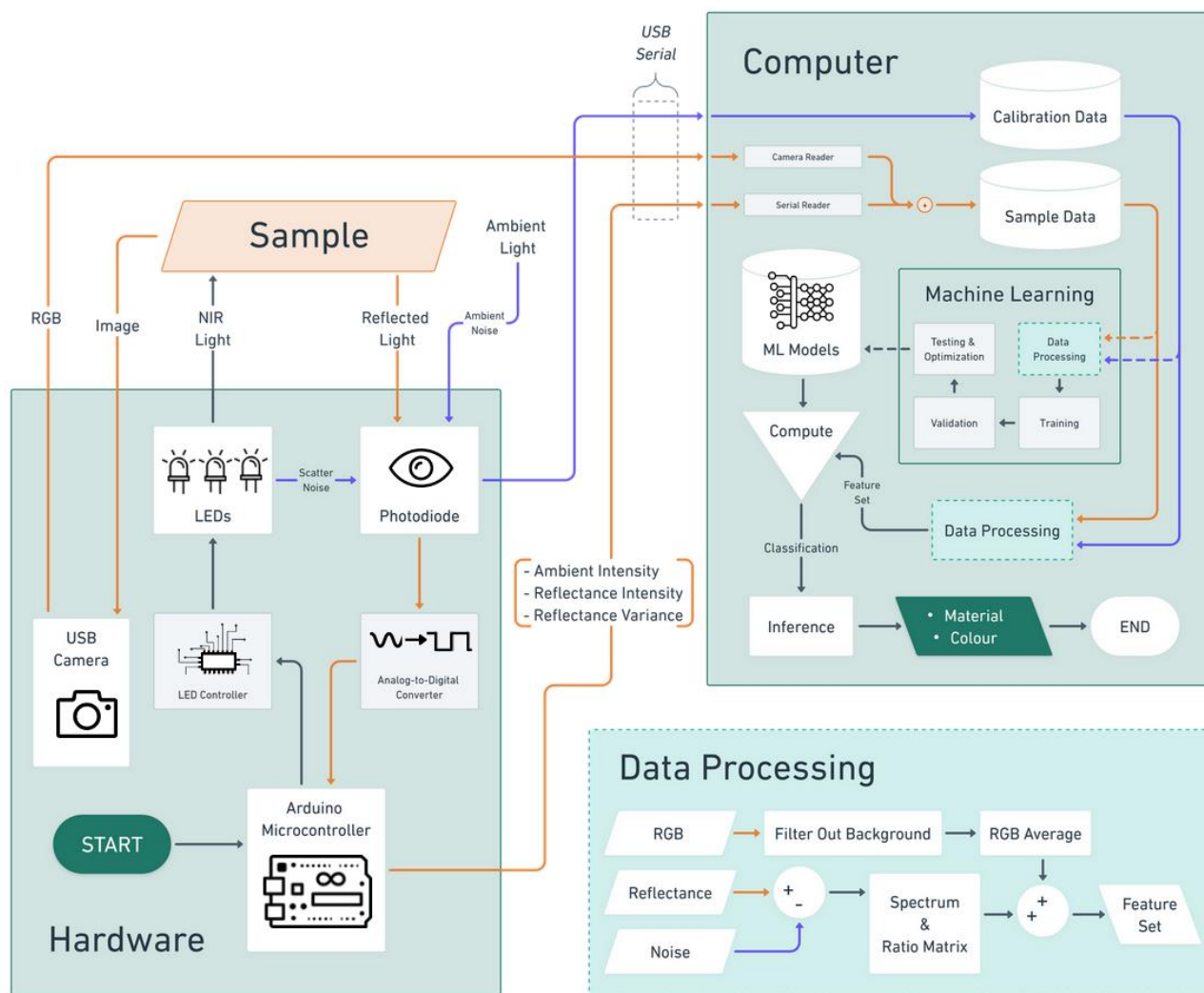


Figure 1. A system diagram detailing the identification system.

3.3 Mechanical Design

An apparatus was designed to house the hardware of the sensor board and camera and satisfy the sizing constraint, corresponding to the maximum size of 3D-printed waste that can be identified and shredded. The apparatus was designed in SOLIDWORKS, and 3D-printed using black PLA. The base plate may be constructed of high-density fiberboard or another readily available material.

The apparatus consists of four parts: a base plate, a contoured cover for the sensor board, an adjustable clamped arm for the camera board, and a hollow frame to provide size guidance. The cover and frame are designed to be attached to the base plate using flathead countersunk M3 screws, which screw in from the bottom of the base plate into plastic hex spacers in the case of the cover or directly into the legs of the frame. The camera arm is clamped to a flange on the cover. The circuit board is suspended inside the cover using hex spacers. The cover has three cut-out sections: one to allow viewing of LEDs at the tail end of the circuit board for verifying the power and error status, one on the side to allow the Arduino to be connected to a laptop, and one at the front where waste samples are placed and scanned.

The front opening, which allows the LEDs and photodiode to scan the sample, was redesigned from an enclosed collar (Figure 2a) to a more open panel (Figure 2b) because the enclosed collar induced excessive reflectance and reduced the reliability of the classification. For future designs, it is recommended that developers investigate the use of a highly absorbent coating on the inside of the collar to reduce interference, and to manufacture the collar from a non-plastic material such as wood to avoid adding noise to plastic identification.

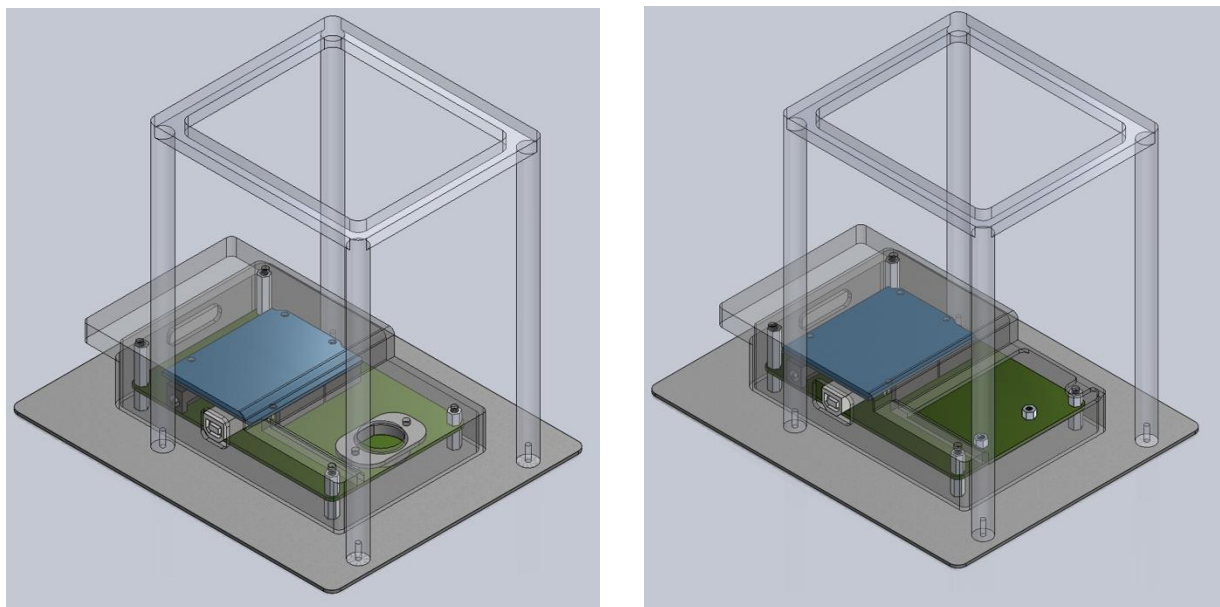


Figure 2. (a) Left: an enclosed cover design with collar and (b) Right: an open cover design with no collar, just standoffs to hold the sample a standard distance from the photodiode.

The dimensions of the hollow sizing extrusion coincide with the size constraints of the input hopper of the Felfil shredder used in 3cycle's recycling line. When a piece of waste is scanned for

identification, the operator must pass the piece through the sizer, which will make it evident if it needs preliminary breaking-down before being shredded.

The camera arm was 3D-printed from an open-source model available on thingiverse.com (HeyVye, 2010) and assembled at the hinges using nuts and bolts. An exploded model of the camera arm is depicted in Figure 3.

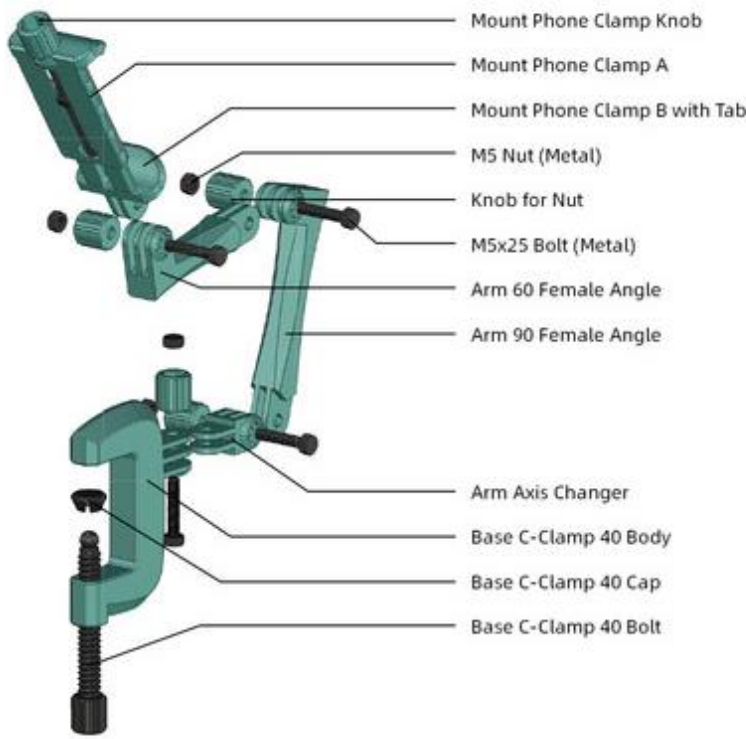


Figure 3. Exploded view of a CAD model of the mounting arm used for the camera board (HeyVye, 2010).

3.4 Hardware & Electrical Design

The hardware and electrical components of the design include an Arduino, a circuit board sourced from the open-source project PlasticScanner (*Plastic Scanner* 2023), and a custom selection of NIR LEDs and a photodiode. The NIR range is ideal for the application, given the goal of low cost and easily accessible components. While near-infrared light can be prone to interference from pigments in the visible spectrum absorbing or reflecting more, near-infrared LEDs are available from common electronics retailers for between 80 cents and 40 dollars each (Digi-key Electronics, n.d.), while far-range infrared lights must be sourced from specialty manufacturers, cost significantly more, and require heat management systems.

The hardware design did not undergo any major revisions since the initial design [1]. The overall hardware architecture can be found in Figure 4 below. However, a second DNIR board was assembled with a different set of infrared LEDs and a photodiode to test a different range of

wavelength and photodiode sensor, in addition to acting as a redundancy measure in the event the original board fails. The wavelengths selected for the second set of LEDs were chosen as such to (1) design for acquisition by constricting to a tighter range which is more frequently detected by commonly available photodiodes, and (2) avoid the 1100+ nm range where absorption by water spikes to reduce the amount of interference caused by moisture in the waste samples. Table 4 outlines the set of LEDs and Table 5 lists the photodiode used for each different board.

Table 4. Wavelengths selected for LEDs in each version of the DNIR module.

Board	LED 1	LED 2	LED 3	LED 4	LED 5	LED 6	LED 7	LED 8
v1.0	850 nm	940 nm	1050 nm	890 nm	1300 nm	880 nm	1550 nm	1650 nm
v2.0	740 nm	850 nm	870 nm	880 nm	890 nm	940 nm	980 nm	1050 nm

Table 5. Photodiodes selected for each version of the DNIR module.

Board	Photodiode	Range
v1.0	0090-3111-185	900* - 1700 nm
v2.0	PD42-21B/TR8	730-1100 nm

* Note that although the reported range is 900-1700 nm, the photodiode still has an effective sensitivity down to 800 nm, and therefore was still able to sense the 850 nm infrared LED.

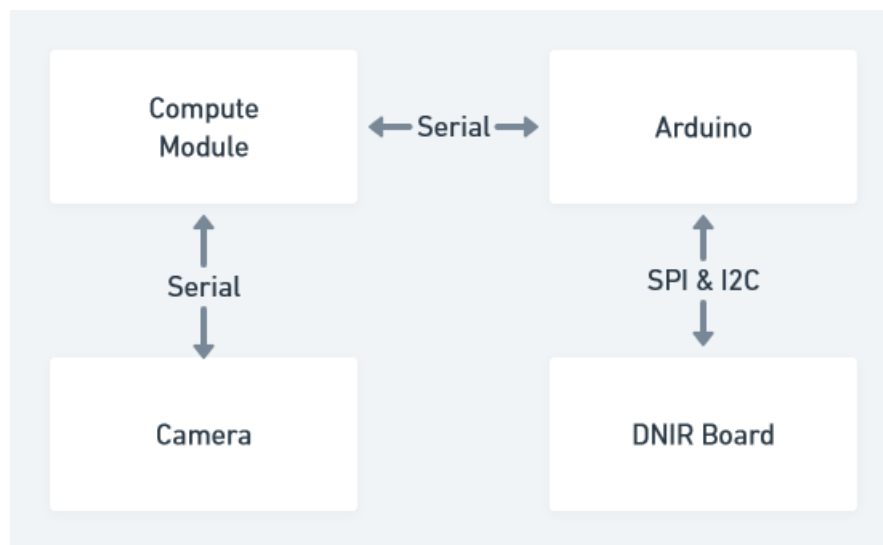


Figure 4. Hardware architecture

3.5 Software Design

The software stack consists of a few key layers. Firstly, the firmware which runs on the DNIR module, which is responsible for collecting the raw data, performs some preliminary calculations and filtering and then serializes the data and sends it over serial to the compute module. Additionally, it initializes all the peripheral chips such as the ADC and LED Driver and monitors the serial port for commands to start its scan operation.

Next, the software backend collects the data from the serial port, then runs it through a custom processing module which finalizes the spectra. There are scripts that automate the data collection, along with utilities to plot and analyze the data. Lastly, a GUI was developed to run and command the entire system through a simple interface which is directly connected to the backend. Noteworthy is that there is an entire machine learning pipeline also connected to this stack. That will be covered in more detail in its own section.

3.5.1 Firmware Design

The firmware was built using a framework, known as PlatformIO, that provides a large suite of libraries for embedded development. It has the Arduino library integrated into it as well, since the MCU of the DNIR board is an Arduino based chip leveraging the existing Arduino libraries' simplified development. The firmware consists of a set of drivers to initialize the ADC, LED Driver along with SPI, I2C and Serial communication. The main loop waits for commands to be sent over serial to tell the DNIR board specific operations to execute. If a "scan" command is received, the board will perform a scan according to the algorithm in 3.6.1 Spectra Generation Algorithm. The data are then sterilized and sent over the serial bus to the host which sent the initial command, a diagram of the firmware is present in Figure 5.

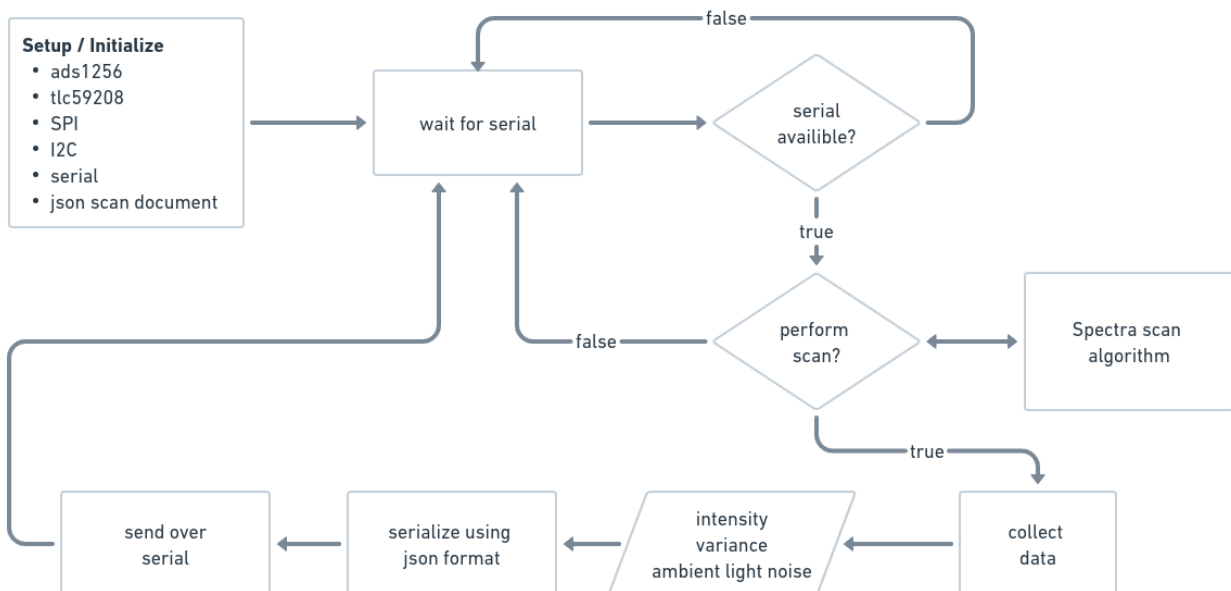


Figure 5. Firmware architecture and procedures

3.5.2 Backend Software Design

The primary components were written in Python using a suite of libraries. The backend consists of a reader module to read both the serial and camera data. The data are fed through a preprocessing pipeline which completes the spectra and extracts the relevant image data. The image data are passed through a simple colour detection algorithm before being passed as an input to the model and the application. Both the DNIR and image data are collected and subsequently fed as input to a trained model. The model performs the inference which outputs a classification based on the selected model, as a few different models were trained with different sets of classifications and for each board version. The output data and classification are then passed to some end application, for our case, this was a GUI. However, these data can be consumed in a variety of ways.

Other scripts were used to plot and visualize the data and perform the data collection tasks independently. Currently, all data are stored locally on the host machine in csv format as for the scope of this project there was no need for a fully integrated database.

A diagram of the software architecture is depicted in Figure 6.

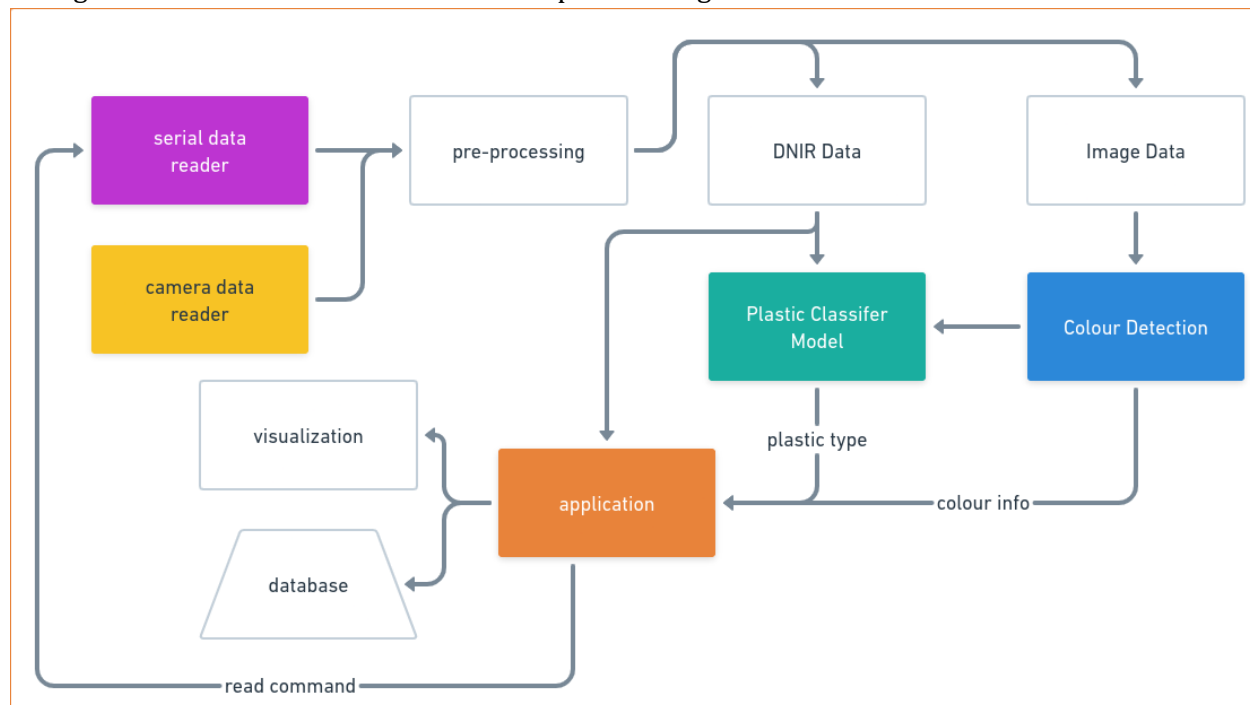


Figure 6. Backend software system diagram

3.5.3 UX/UI Design

A graphics-user interface (GUI) was built as the application block in Figure 6 above as the final layer to provide an easy interface for users to interact and view data. The GUI was designed in Python using a GUI library known as tkinter and customtkinter. The GUI was built on top of the backend described above and provided the top-level control along with the ability to view the data.

A GUI was built as an end application since it provides a user interface which displays data and outputs in a concise fashion for the user. Further, it provides a simple control interface for the user to interact and operate the system. For the current end application, a human operator is required, so this design is tailored for a human operator in mind. A mock-up of the GUI design is shown in Figure 7.

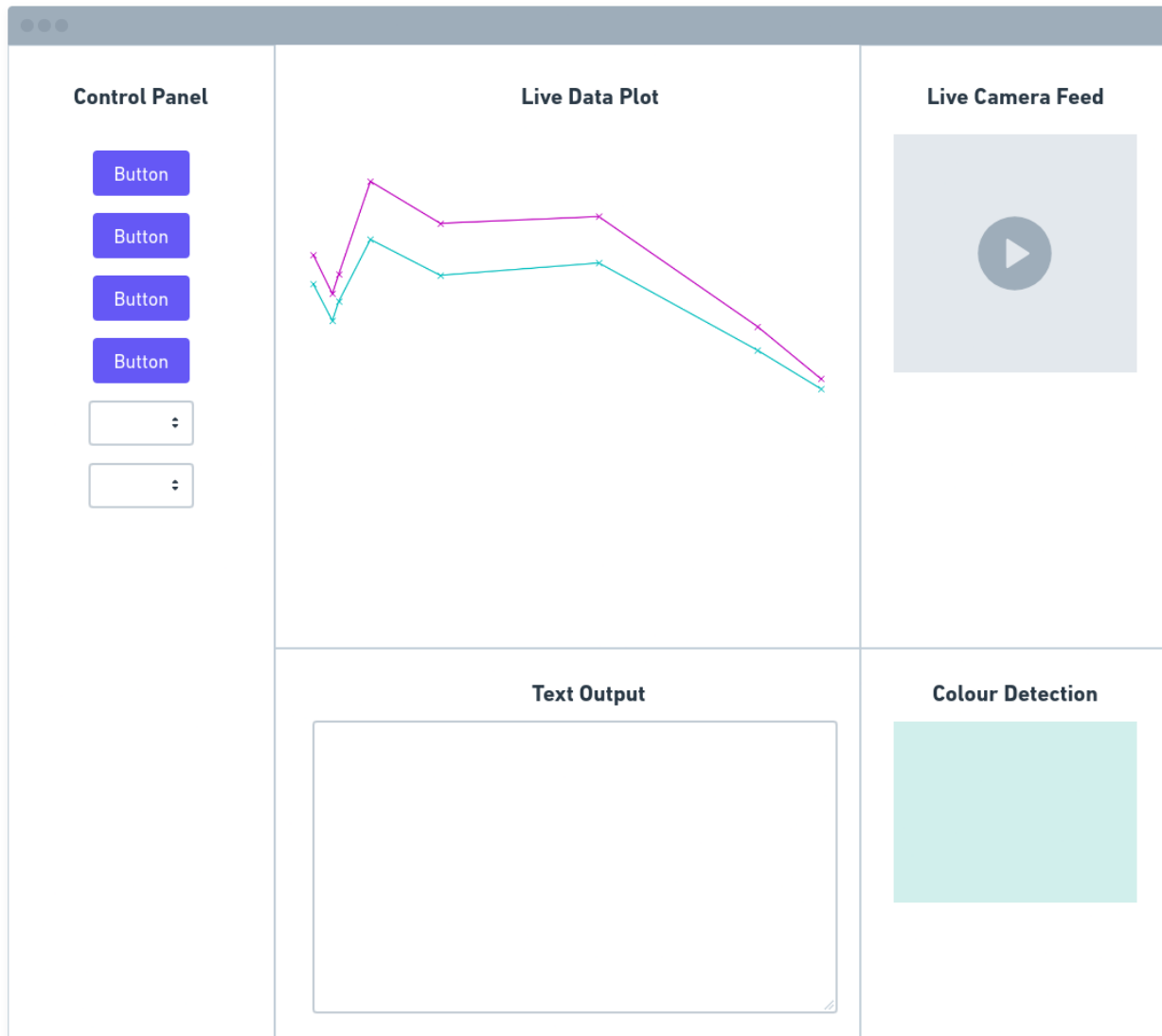


Figure 7. Graphics-user interface (GUI) mock-up.

3.6 Algorithms and Machine Learning Design

To generate the spectrum and capture the colour from the image data, a set of algorithms were developed. To perform the classification of the plastic type, a different set of approaches could have been utilized: from heuristics, a custom algorithm, or machine learning.

Machine learning was chosen for this application for several reasons. Firstly, the data are highly dimensional with a considerable amount of noise. Next, the spectra varied between the different

board types and were evolving during development. Lastly, because the data were constantly evolving and dynamic, a framework that could easily evolve was preferred.

To this last point, with a heuristic or algorithmic approach, altering an LED on the board or modifying the spectra generation would require altering the classification algorithm. Further, it would likely differ between different board types. Since the data are highly dimensional, it would be difficult to visualize the data without using dimensionality reduction techniques.

To accommodate all these factors, a machine learning approach was preferred. Firstly, machine learning is well suited to highly dimensional, noisy data. Further, once a dataset is developed and the framework is in place, it requires minimal effort to re-train a model which uses a different set of input and generates a different set of outputs. As a result, this allows for fast iteration and development as different models can be quickly trained and tested; the input/outputs can be altered without having to modify the internal structure of the model. Thus, a machine learning pipeline was built to take the collected raw data, pre-process them and perform feature engineering before feeding them through training and validation which tested many different models and selected reported the results. Additionally, methods to optimize the model hyperparameters were created to further optimize selected models, along with a synthetic data generation script. From initial scans and testing, it was determined that it should be viable to minimally differentiate between ABS and PLA. From Figure 8, we can see that ABS is contained to range, across all colours between white and black to the region within the red, whereas PLA is contained to the region within the black. This visualization indicates that the plastics are different independent of colour and can be differentiated.

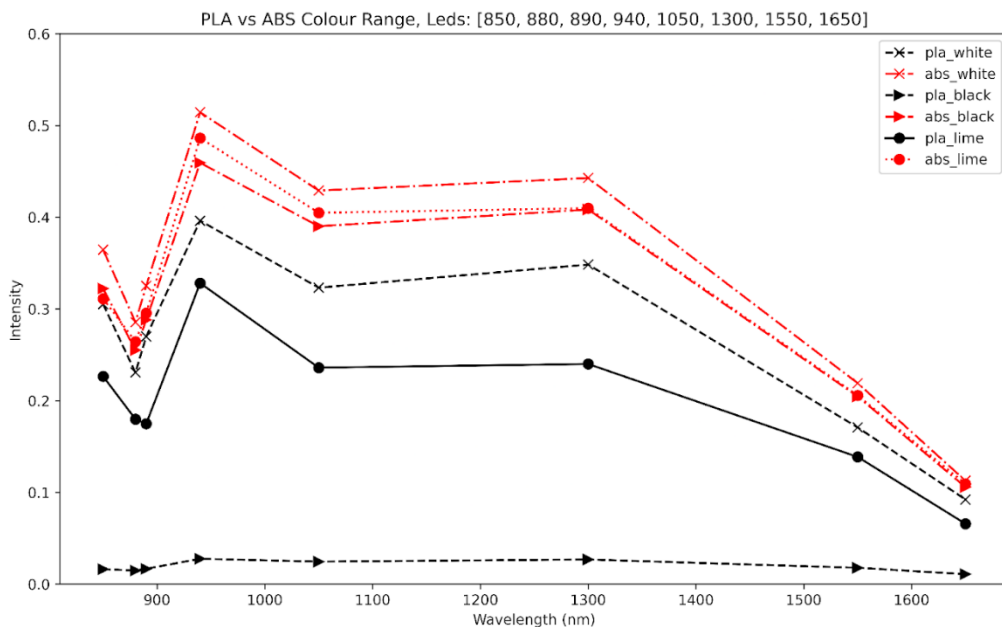


Figure 8. PLA (red) vs ABS (black) reflectance readings for white, lime, and black samples.

3.6.1 Spectra Generation Algorithm

Multiple forms of spectroscopy exist, each having their own challenges. However, one of the primary challenges is the accurate interpretation of the data, which requires a deep understanding of the physics behind the measurements. Additionally, there can be interference from other molecules or substances within the sample, making it difficult to identify specific features in the spectrum. Another challenge of spectroscopy is the need for appropriate instrumentation since the sensitivity and resolution of the instrument can affect the data quality.

Dr. Simarjeet Saini, a professor in the Department of Electrical and Computer Engineering, provided the following lessons in spectroscopy which proved very helpful in the design of our project.

In the case of reflectance-based spectroscopy, there are two forms: diffuse and surface reflectance. Diffuse reflectance is better at capturing the characteristics of the core functional groups, but its signal has a much lower intensity since a significant amount of light is lost to absorbance. Surface reflectance uses a higher intensity signal to capture the resonant peak characteristics of these core functional groups in the material, but these peaks are less distinct than looking directly at the core functional groups. The DNIR board is primarily dominated by surface reflectance, which provides enough data to be acceptable for this specific application of differentiating between 3D-printed materials.

Due to the nature of the signal, a couple different sources of noise will be always present. These include ambient light from the environment, LED scatter - since the LEDs and the photodiode lie on the same place and the LED emits light in a cone like shape, some of the light from the LED will be directly absorbed by the photodiode or may reflect off some other surface first on the board itself, and lastly system noise. System noise refers to the additional electrical signals present in the ADC measurements. Signal averaging was used in the algorithm to minimize this noise. Further, it was verified that the signal to noise ratio for each LED was sufficiently high, at around 10.

To capture the ambient light for each reading taken for a LED, a reading was taken with all LEDs off. The ambient light was averaged and returned along with the intensity and variance for each LED. Lastly, for the LED scatter noise and to account for the ambient light without a sample present, it was determined that for each set of scans a calibration was required. The calibration only needed to occur once per session or if the ambient light conditions changed significantly. The calibration was simply a scan with no sample on the board in the open environment.

These sources of noise - calibration for the scan session and ambient for each scan - were then subtracted from the raw intensity values during post processing. Additionally, if any intensity value with the noise subtracted was less than zero, it was set to zero to keep values positive. Any such value has effectively more noise than signal and should be treated as zero signal. Most of the algorithm, as represented in Figure 9, is executed on the DNIR board during the scan process, with the final step of removing noise taking place on the host machine since it needs to reference the appropriate calibration for the current scan. Each calibration was identified with a date and an ID, and each scan recorded the appropriate calibration ID it should reference.

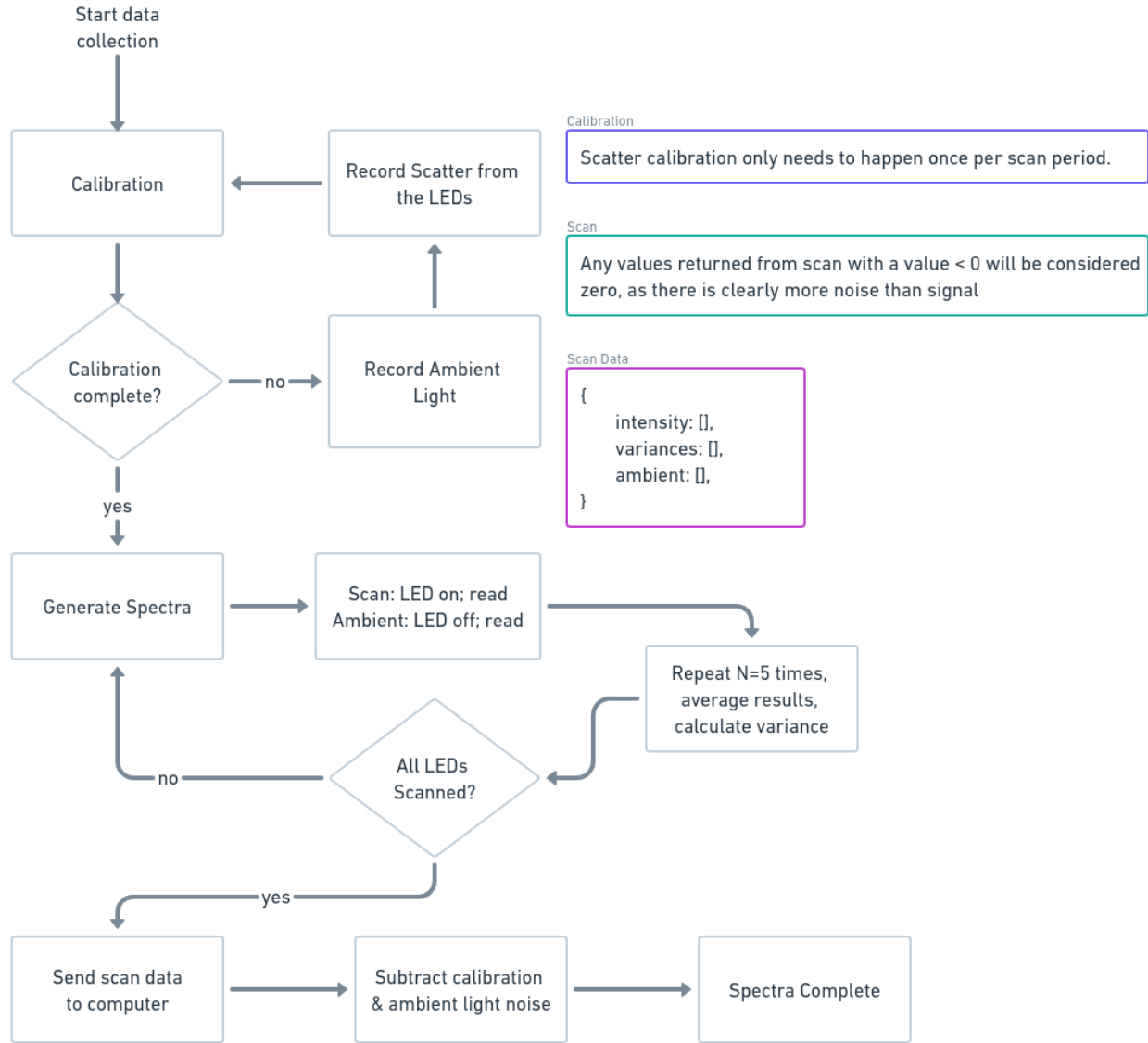


Figure 9. Calibration and noise-filtering procedure.

3.6.2 Colour Detection Algorithm

Initially, the colour detection was thought to be an on-going process that would also use object detection to record the colour in an automated fashion. However, for this project, the scope was reduced to have the colour detection be a request-based process that executed based on user input. A camera was considered the preferred colour recording method, instead of a colour sensor, for several reasons.

First, a colour sensor is a point sensor which can only measure a point or a small area. Since a variety of shapes and sizes of samples were anticipated, it was difficult to determine a single point that would be consistent other than directly where the LEDs and photodiode were located. This posed a problem though since any colour sensor added here would take up space and may interfere with the LEDs and photodiode. A camera was deemed better since it can effectively detect colour of

a larger area rather than a singular point, making it more robust to the diverse possibility of geometries of 3D-printed samples. Additionally, it can be mounted high above the scan area preventing interference with other parts of the process. Lastly, it gave the design the hardware capability to be automated later by using object detection to identify when a sample is present and then perform a scan automatically.

The algorithm (Figure 10) would get a set of N frames, where each frame is a single frame of video and consists of a set of matrices of red, green, and blue values for each pixel. Then, the camera was positioned such that the center was aligned with the center of the scan area. For each frame, only the area around the center was taken. This area was the size of the hole required for all the LEDs and photodiodes. Therefore, it was known that this would fully encompass the sample as it was a requirement that the sample be large enough to fully cover this hole. This effectively filtered out the background image, leaving only the pure sample image frames. Then, the individual pixel values for the red, green and blue components were averaged across all N frames giving the mean red, green and blue values, which corresponded to the mean colour of the sample.

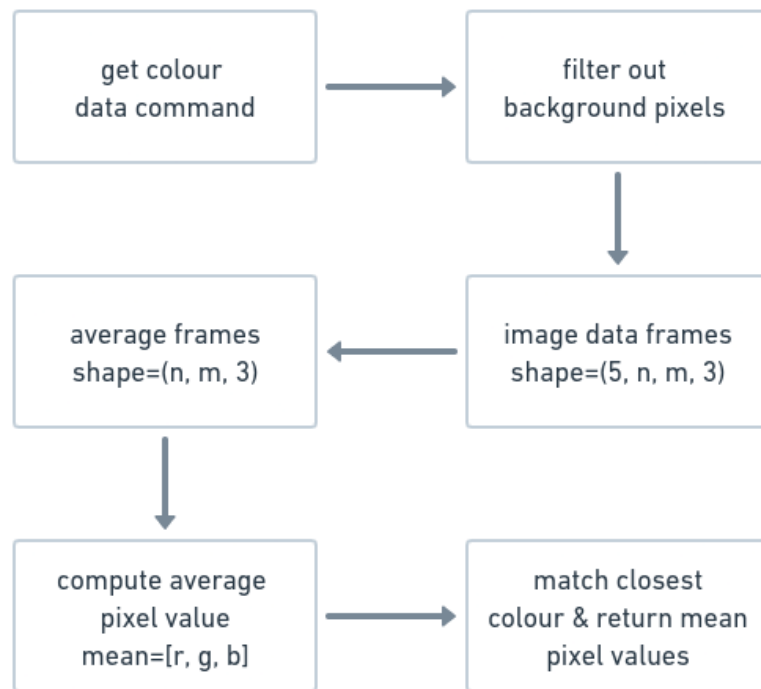


Figure 10. Computer vision procedure for colour identification from camera input.

3.6.3 Machine Learning

Initially, the intent was to use an algorithmic or heuristic based approach to classify the plastic type based on the data. However, as discussed previously, machine learning was determined to be the most effective strategy.

The first component was determining the contents within the feature vector. Feature vectors are used to represent numeric or symbolic characteristics, called features, of an object in a mathematical way. Machine learning algorithms typically require a numerical representation of objects for the algorithms to perform processing and statistical analysis (*Feature Vector / Brilliant Math and Science Wiki* (n.d.)) eight processed intensity values representing the spectra of the sample. Next, through experimentation, calculating the ratio of every intensity value to every other intensity value was found to improve accuracy (Straller, (2019)). This produced an 8x8 matrix of values which was flattened to a vector of 64 values. Lastly, the mean red, green, and blue values were added to the feature vector. A schematic representation of this algorithm is shown in Figure 11.

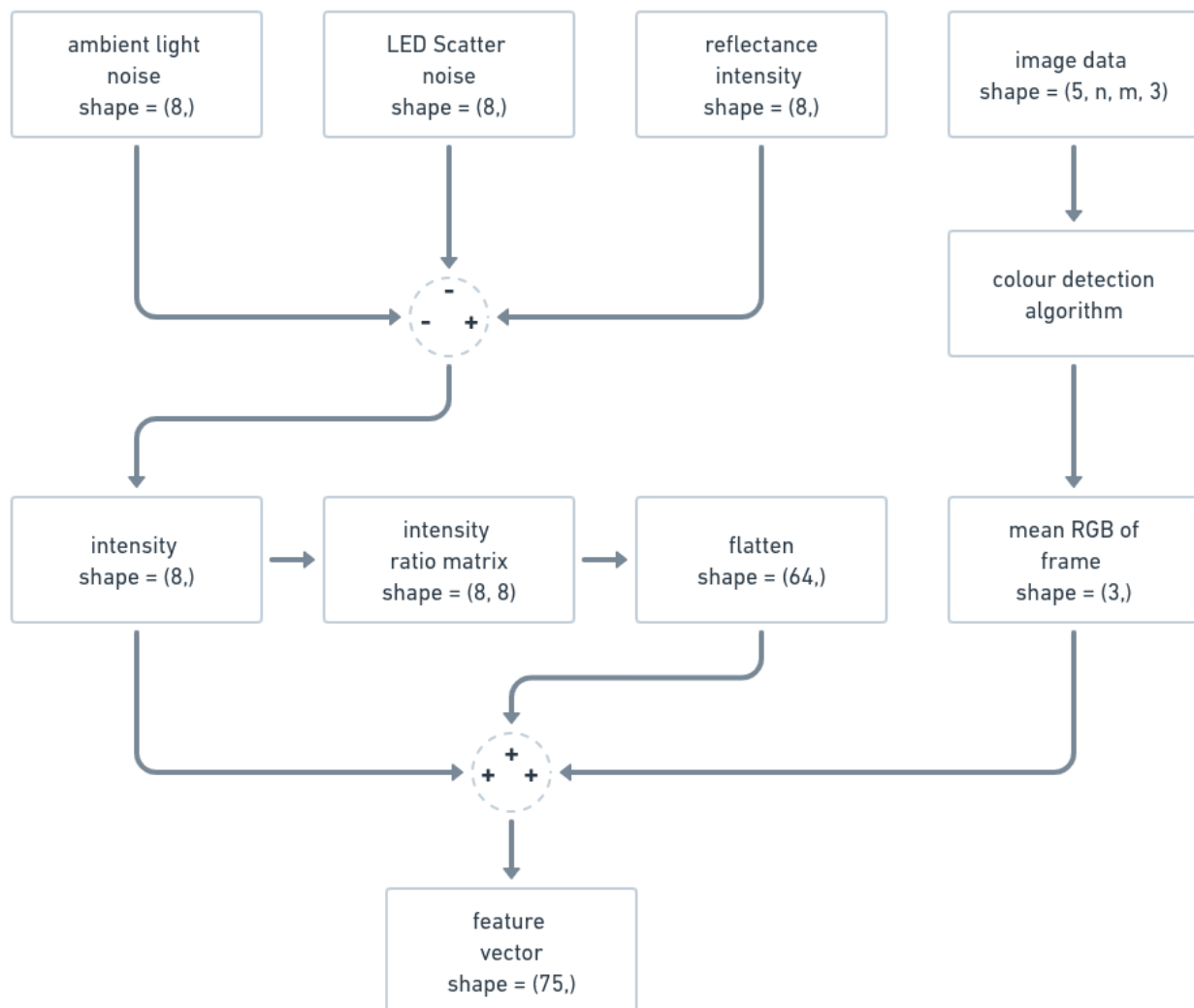


Figure 11. Feature set generation procedure.

Initially, the mean colour of the sample, in the form of the red, green, and blue values, was not considered necessary based on Figure 12 since ABS and PLA were both distinctly separate from each other. However, upon investigating other materials, it was found that other similar materials

would overlap this range. Figure 12 illustrates how PETG spans the ABS and PLA range. In particular, PETG red is similar to PLA red and PETG orange is similar to PLA white. This overlapping was not unique to PETG and was similar to other plastics as well. However, overlapping spectra generally did not have the same colour. Therefore, colour could be used as another dimension of data to help differentiate the spectra.

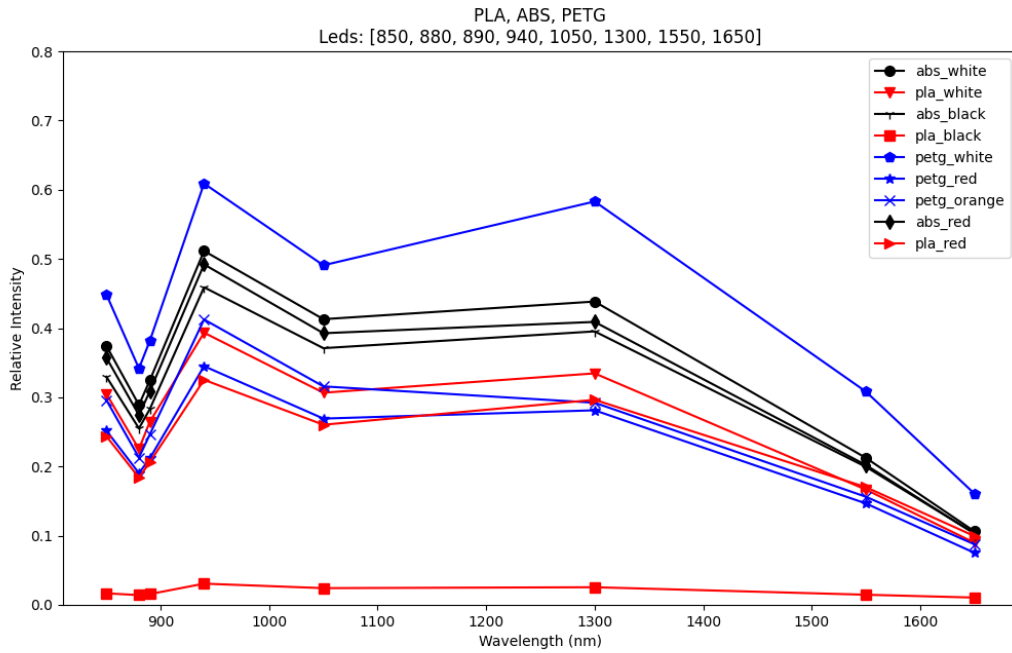


Figure 12. PLA vs ABS vs PETG spectra to show how other plastics overlap with PLA and ABS in certain areas.

With the feature vector determined, a pipeline (Figure 13) could be built to create a dataset and train a model to perform classification. A dataset was collected using 100 samples of different pieces of PLA, ABS in various colours, along with some PETG, types 1-6 and other plastics, and non-plastic materials. The data were split using an 80:20 training: validation split. The data were trained on a set of various models available in Figure 14. The model with the highest validation accuracy was selected; its hyperparameters and training information along with a serialized version of the model was stored. Each model was optimized using Halving Random Search, a technique to further optimize a models hyperparameters.

The trained models can be selected by the end application, given an input vector and then run inference to create a prediction. Different models were trained for each different version of the board and for each board a model trained on a different set of classifications was generated.

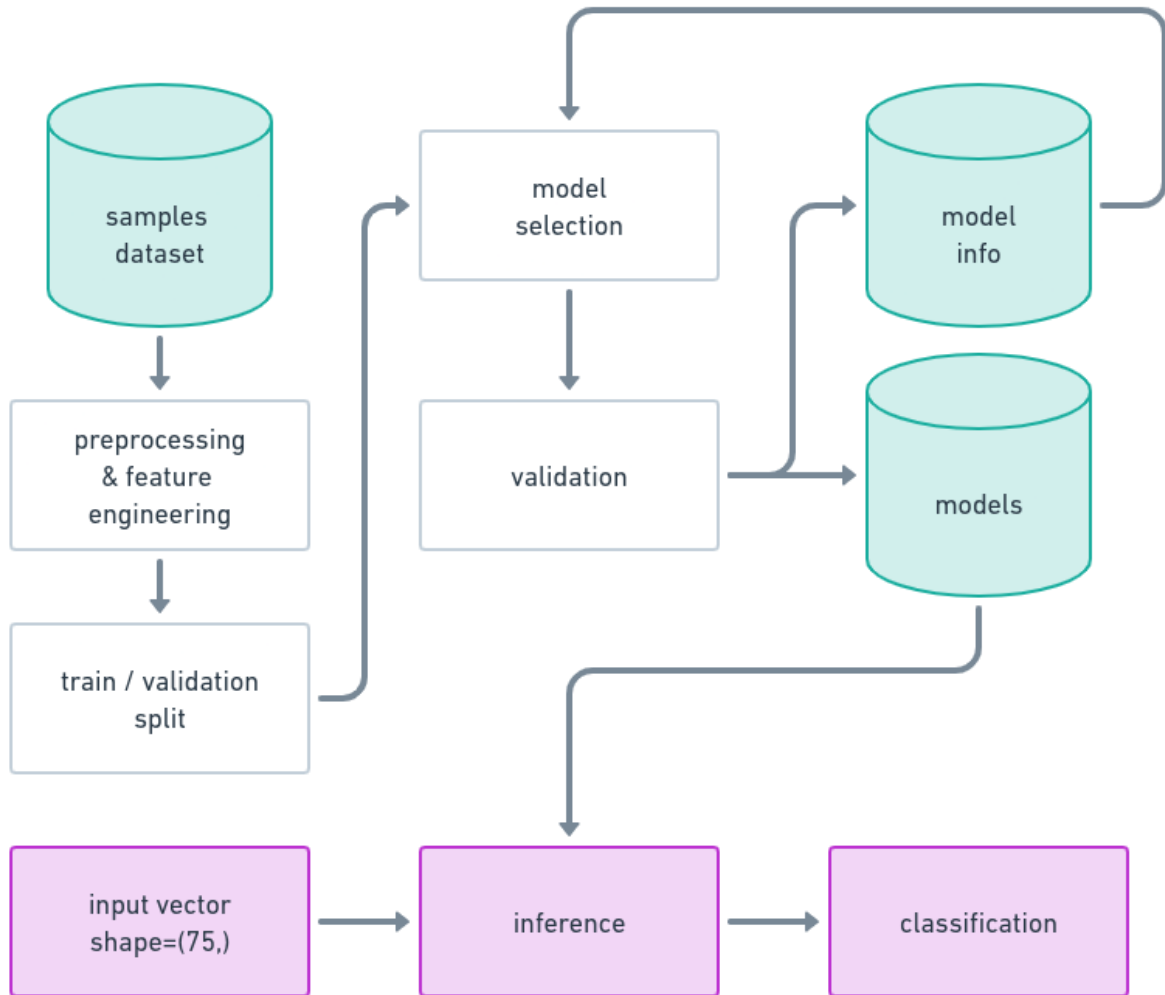


Figure 13. Machine learning pipeline system diagram

```

1 # -----[ Select Models ]-----
2 names = [
3     "Decision Tree",
4     "Random Forest",
5     "Bagging Classifier",
6     "Extra Trees Classifier",
7     "Gradient Boosting Classifier",
8     "Voting Classifier",
9     "Histogram Gradient Boosting Classifier",
10    "AdaBoost",
11    "K Nearest Neighbors",
12    "Linear SVM",
13    "RBF SVM",
14    "MLP Classifier",
15    "QDA",
16 ]

```

Figure 14. Names of models trained and tested in the machine learning pipeline.

Table 6. Summary of selected trained models

Board Version	Type	Classifications
v1.0	Gradient Boosting Classifier	ABS, PLA, Empty
v1.0	Gradient Boosting Classifier	ABS, PLA, PETG, Plastics, Non-Plastics, Empty
v1.0	Quadratic Discriminant Analysis	ABS, PLA, Empty, Other
v1.0	Random Forest	ABS, PLA, Empty
v1.0	Support Vector Machine	ABS, PLA, PETG, Plastics, Non-Plastics, Empty
v2.0	K Nearest Neighbors	ABS, PLA, Empty, Other
v2.0	Histogram Gradient Boosting Classifier	ABS, PLA, PETG, Plastics, Non-Plastics, Empty

3.7 Reformulation Summary

Three aspects of the design underwent reformulation when problems were discovered during prototyping: the cover enclosing the DNIR sensor board, the set of wavelengths selected for spectroscopy, and the method of spectrum collection. All three design choices were related to interference when scanning.

The tight enclosure for the LEDs and photodiode in the cover and collar were made of PLA, and this caused the classifier to output many false positives for PLA samples. The project timeline did not allow for remanufacturing of the cover and collar out of non-plastic materials, so the enclosure was redesigned to be more open (Figure 2b) to reduce reflectance noise bouncing off the cover and collar.

Professor Simar Saini advised the team of the likelihood that moisture was interfering with preliminary NIR scans, as water has high reflectance above 1100 nm and especially at 1300-1400 nm. Accordingly, a new set of LEDs was selected to avoid this range, as reflectance with moisture would not provide useful data for differentiating PLA and ABS, and introducing a dehydrator to 3cycle's recycling line was not deemed feasible within the project timeline.

The method of spectrum collection for the DNIR module originally performed only one scan to collect the reflectance for each LED. To introduce more robustness and eliminate random noise, the method of spectrum collection was changed so each LED was flashed 5 times and the data were averaged.

4.0 Engineering Verification & Validation

4.1 Lab Experiments

4.1.1 Spectrometry Research

Dr. Simar Saini, a professor in the Department of Electrical and Computer Engineering, provided expert guidance on spectroscopy. Initial readings with our board showed results near zero for a certain range. Dr. Saini explained that the plastic used for the readings likely contained water with hydroxyl bonds present on the surface. Water absorbs a lot of the wavelengths between 1250 and 1500, with the largest peak at 1380 nm, which could cause low readings in the mid-range spectrum (Saini, 2023). Dr. Saini advised us to use wavelengths far away from those water wavelengths (Saini, 2023).

Dr. Saini explained different ways of doing light measurements. Diffuse reflections consist of shining lights away from the detecting spot, but rather, shining light into the material and letting it scatter around. This is best done after transmission. The second way is to shine light exactly where the measurements are being taken, which provides a first reflection of the surface. This reading provides information, but it is not as strong. The preferred method is transmission because the presence of a distance is known. This has led to its use in O2 finger meters (Saini, 2023).

Our initial FTIR board was measuring with mid-wave infrared, near 7000 nm. However, the lowest wavelength for the FTIR machine in Dr. Mekonnen's lab was 4000 nm. The discrepancy between the two challenged their compatibility.

Sample thickness affects absorbance a lot until the point is reached where thickness is so great it no longer matters if one sample is larger (Saini, 2023). Therefore, given our use of samples of very different thicknesses, surface reflectance is likely more suited for our application. However, surface reflectance readings may be impacted by the oil or moisture of the surface of plastics. This may be remedied by washing and dehydrating the plastics before taking spectroscopy readings. Moreover, washing and drying is a standard in professional plastics processing, and would improve the quality of the final recycled 3D printer filament (Saini, 2023).

Dr. Saini used his spectrometry meter to take readings of PLA and ABS. Figure 15 shows the results from the first series of readings with different coloured samples.

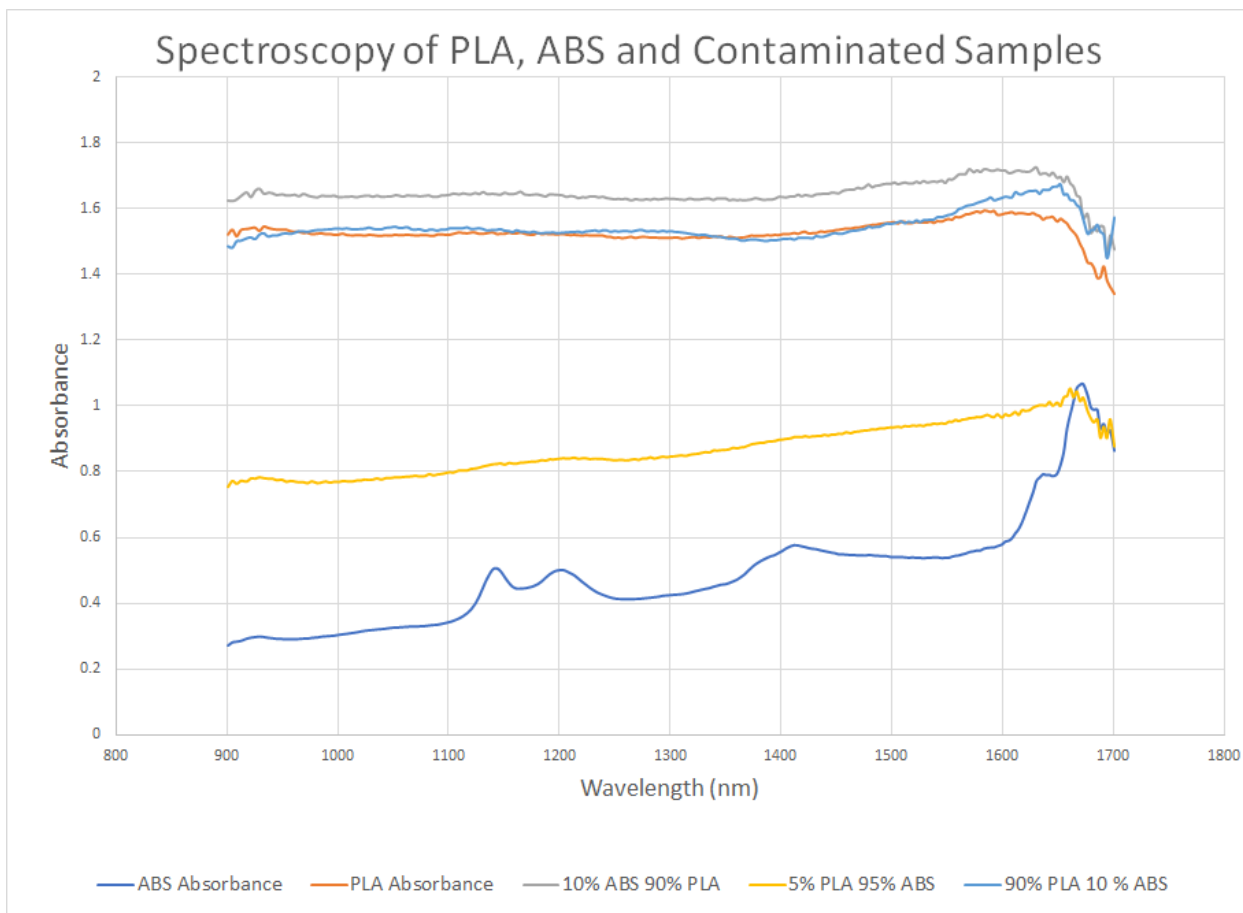


Figure 15. Spectrometry readings of PLA, ABS, and contaminated samples.

shows the difference in the absorbance determined by taking a spectrometry reading of black PLA, red ABS, and contaminated samples (one that was grey and the other purple). The 'pure' PLA sample and the contaminated PLA samples were seen to have nearly complete absorbance with an almost horizontal curve. This is called broadband absorption (Saini, 2023). The ABS sample, however, showed clear peaks around 1200 nm, 1400 nm and 1650 nm. The ABS sample contaminated with 5% PLA showed an absorbance closer to the values for ABS but without the same peaks.

To determine the impact of the pigment on the PLA and ABS spectra, spectrometry readings were retaken using PLA and ABS samples of the same colour. Figure 16 shows the results.

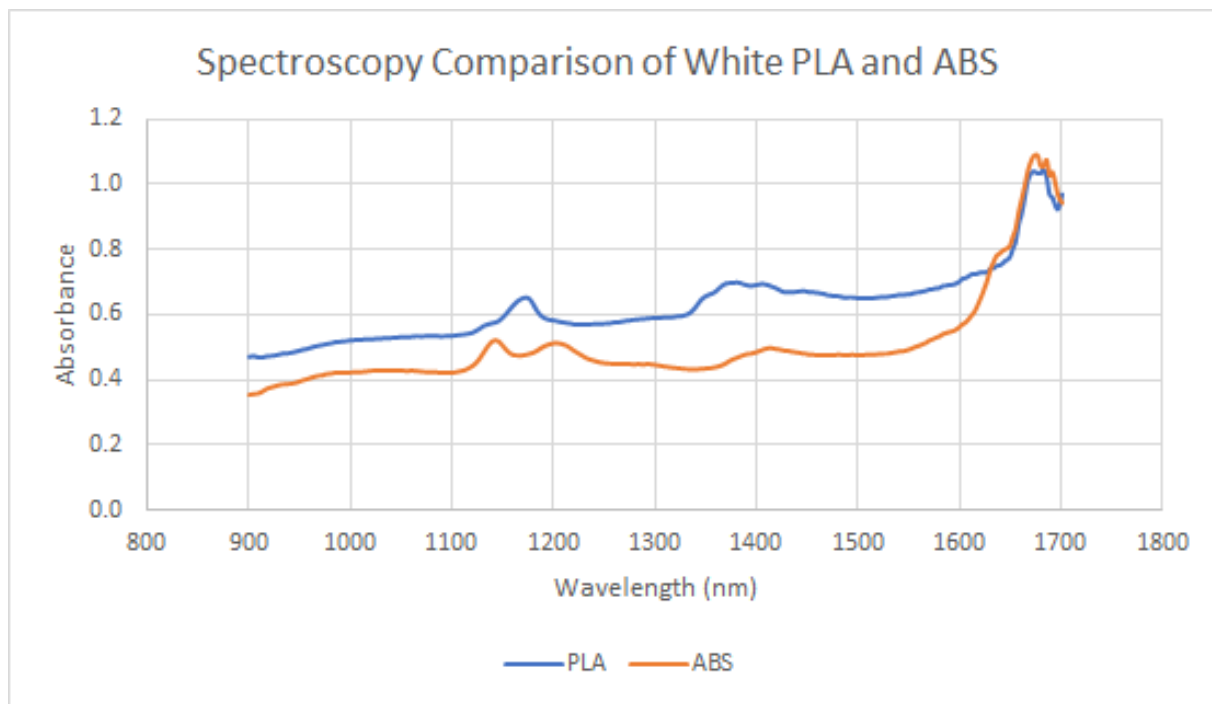


Figure 16. Spectrometry readings of PLA and ABS of the same colour, white.

In the plot of absorbance vs wavelength, white PLA and ABS are seen to have different absorbance curves over the range of measured wavelengths. The difference is most noticeable around wavelengths of 1140 nm, 1175 nm, 1210 nm and 1400 nm. These would be good target areas for LEDs (Saini, 2023).

4.1.2 Plastic Recycling in the Mekonnen Lab

Using the batchmixer in Dr. Tizazu Mekonnen's lab, waste samples of PLA and ABS were recycled. The waste PLA was shredded and then fed into the batchmixer heated to 170 °C and mixed at 60 RPM. After the torque had stabilized, the sample remained in the batchmixer at a constant temperature for 6 minutes. Then, with the PLA sample still inside, the mixing was stopped and the batchmixer was cooled to 60 °C. The batchmixer was heated again to 170 °C, the sample was left in the batchmixer for 6 minutes after the temperature stabilized. Then, the sample was removed from the batchmixer and then cooled. The same process was used for ABS. However, the batchmixer was heated to 190 °C, cooled to 80 °C and reheated to 190 °C. This meant two cycles of recycling were also performed on ABS.

This process simulates two cycles of recycling with an anticipated third cycle occurring when the material is melted for filament extrusion. This allows for the degradation to be examined to determine the maximum extension of the material's useful life for 3D printing. Visual observations of PLA and ABS that has undergone two heating cycles show visible signs of degradation. PLA (Figure 17a) had a color change from black to white. The material was also no longer smooth and

shiny but rather textured and matte. ABS (Figure 17b) experienced no change regarding its lustrousness or texture, but the color changed from white to yellow.



Figure 17. (a) Left: black PLA with grey discoloration and (b) Right: white ABS with yellowing discoloration after both underwent simulated recycling in the batchmixer.

Optical examination through FTIR can provide information regarding any molecular degradation that occurs. The spectrum of recycled PLA (Figure 18) does not appear to be altered molecularly as all characteristic peaks are still present. The only evidence of change is the peak at $\sim 1750 \text{ cm}^{-1}$. In virgin PLA this peak is smooth, whereas in recycled PLA the peak has a 'shoulder' indicative of contamination or degradation. ABS did seem to undergo changes to its molecular composition because of recycling. The spectrum of twice recycled ABS is missing a characteristic peak at $\sim 1600 \text{ cm}^{-1}$ and had a single peak around 1750 cm^{-1} compared to the double peak of virgin ABS (Figure 19).

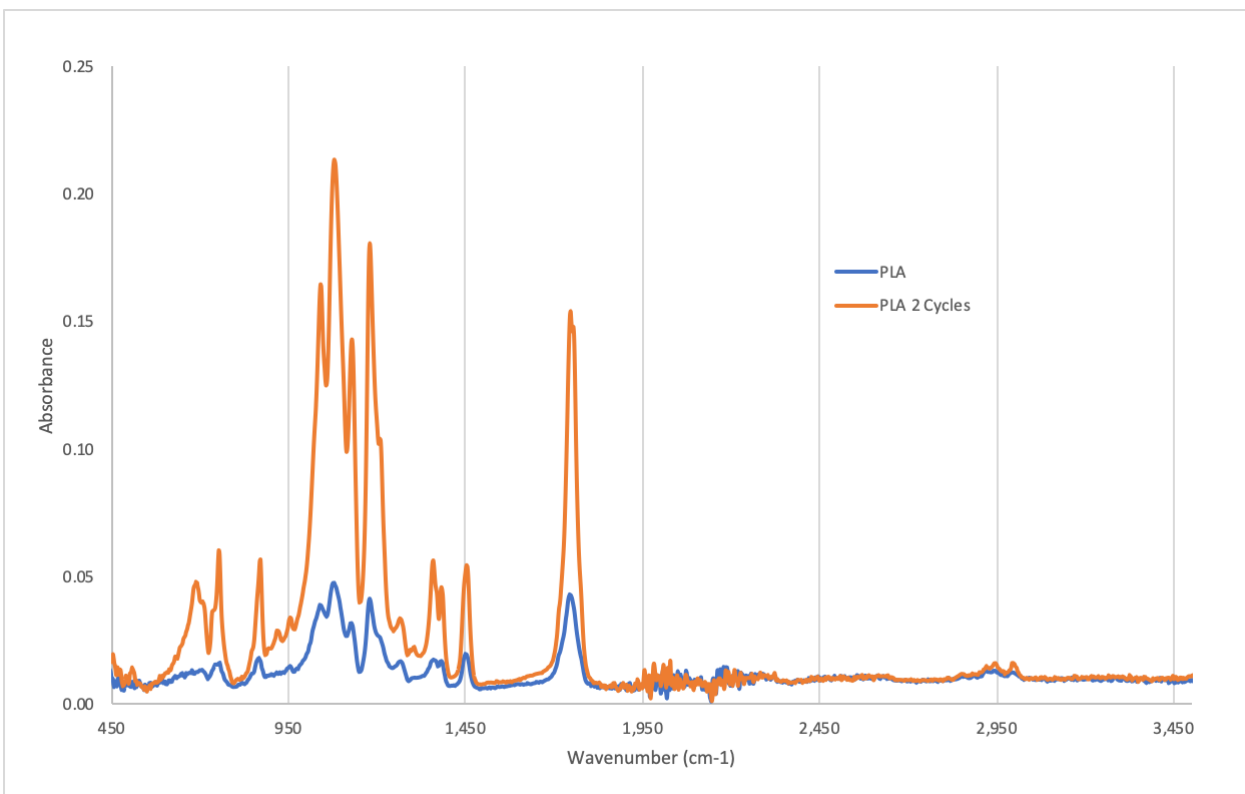


Figure 18. Spectrometry of virgin PLA and twice-recycled PLA.

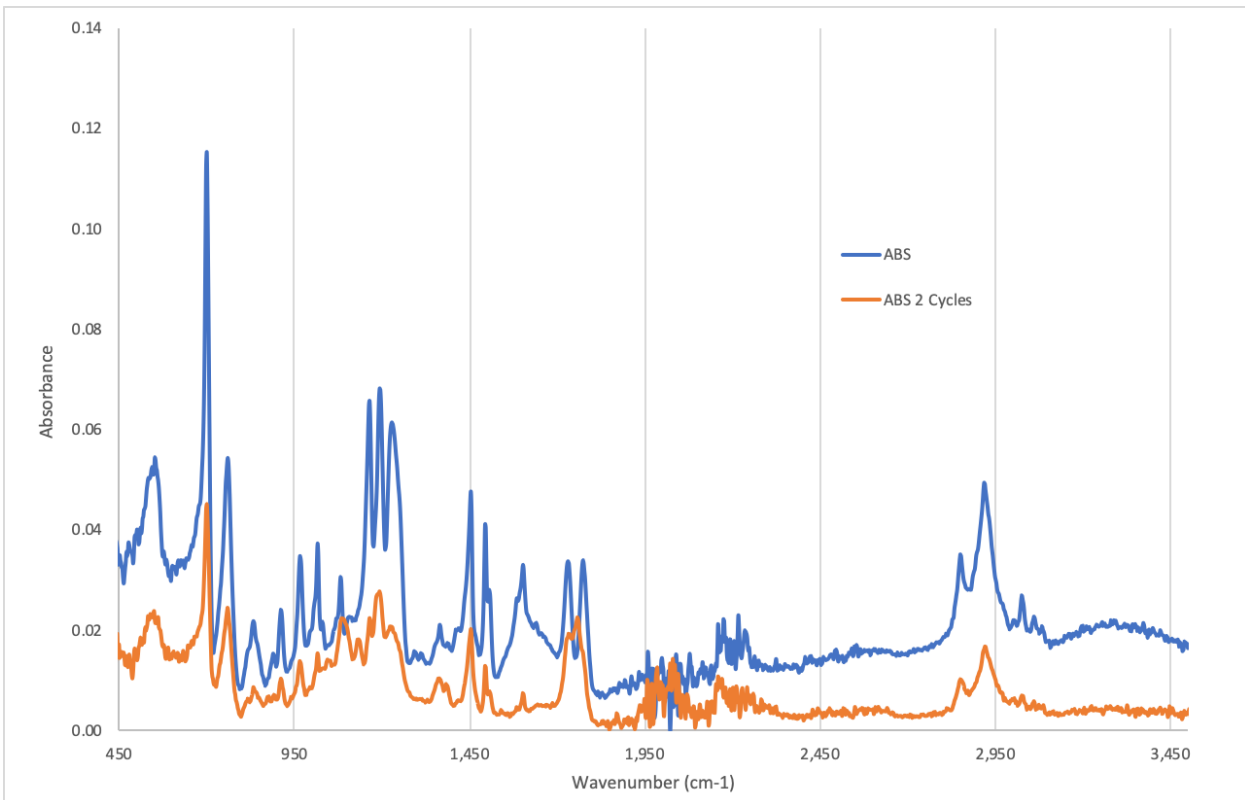


Figure 19. Spectrometry of virgin ABS and twice-recycled ABS.

4.1.3 Tensile Results of the Recycled Filament

After one cycle of recycling, which consists of shredding, extruding, and spooling filament from PLA waste, it is ready to be printed and its mechanical properties can be tested. Similarly to the tensile tests performed with virgin PLA, five dog-bone samples were 3D-printed according to ASTM standards and the test was performed with a 10 kN load and pull rate of 10 mm/min. The stress-strain curves of virgin and recycled PLA can be found in Figure 20 where R-PLA indicates recycled samples. Table 7 contains other mechanical properties of recycled PLA and how they compare to that of virgin PLA.

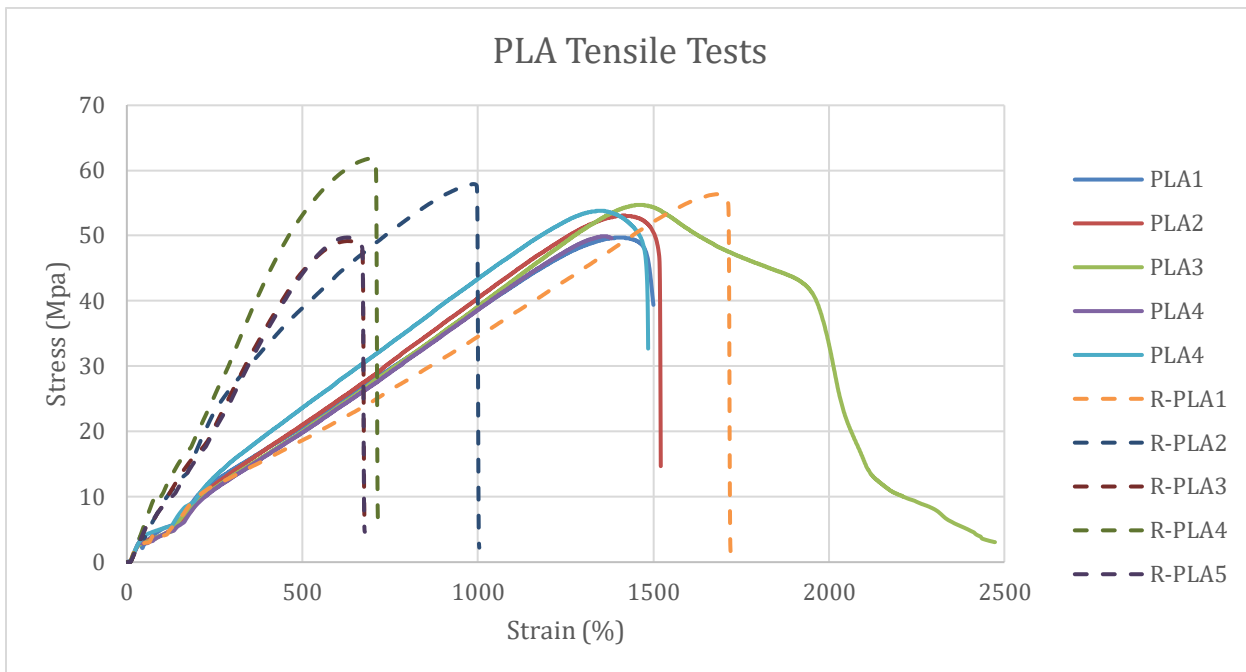


Figure 20. Tensile test results of virgin and recycled PLA

Table 7. Mechanical property comparison of virgin and recycled PLA

Name	Young's Modulus	Ultimate Tensile Strength	Strain at Break	Time of Break
Unit	GPa	MPa	%	sec
Virgin PLA	0.73714	52.2300	11.8701	15.672
Recycled PLA	1.02674	54.9871	7.15043	9.442
% change	39%	5%	-40%	-40%

Unexpectedly, the recycled samples display a slight increase in ultimate tensile strength. This may be due to differences in temperature and humidity during printing and/or during testing. The recycled PLA displayed significantly reduced elasticity, percent strain, and time to breaking. When commercializing this process, the altered performance of the filament will have to be communicated to consumers and it will likely have to be sold at a lower cost than virgin filament. Alternatively, there is the option to add a certain amount of virgin PLA when making filament to achieve acceptable mechanical properties.

4.1.4 Recycled Filament Making in the Velocity Lab

Using the extruder and spooler purchased by the greater 3cycle team, Team 10 experimented with taking shredded 3D printer waste samples and extruding them into filament for 3D printing. The following challenges were experienced.

Firstly, the shredder did not work out of the box. The procedures recommended by the user manual and customer service did not resolve the issue, so the device was carefully opened for inspection. A wire connecting the start button to the control circuitry was disconnected on one end. Reconnecting this wire resolved the issue.

It was initially hard to match the speed on the spooler to that of the extruder to avoid a build-up and knotting of material exiting the extruder. The motor and spooler were also not working together which meant the spooler would not turn independently. As well, the recycled filament had an inconsistent diameter. (The spooler has a built-in meter to provide live measurement of the filament diameter. We observed that the diameter was inconsistent.) Changing some settings on the spooler allowed a consistent diameter around 1.2 mm to be obtained. However, this was still considerably below the target diameter of 1.75 mm, which represents the standard filament diameter from industrial manufacturers.

After a lot of trial and error, we managed to obtain several meters of filament with a consistent diameter between 1.65 mm and 1.80 mm: a long enough length to print into dog bones for tensile testing.

The diameter of filament produced is highly variable with fast pull speeds making the filament too thin and low pull speeds leading to thick filament. Ultimately, slow pull speeds have a greater impact on production as it both reduces throughput and can lead to a build-up and kinking of melted plastic at the nozzle of the extruder. Kinks or knots in the filament cannot be fed through the support rings on the fans and the process must be reinitiated. There are countless variables that determine the filament diameter with only three being controllable: the pull speed, the RPM of the extruder screw and the extruder temperature. The pull speed of the spooler can only be controlled on 'manual' which is the preferred mode of operation since 'soft' and 'hard' modes automatically adjust pull speed according to diameter readings. However, since the spooler operates independently of the extruder, it has no means of knowing the rate of extrusion and adjustments are purely based on diameter readings. Even when manually selecting the pull speed, the diameter is still inconsistent due to the extruder. The RPM is correlated to the rate of extrusion, but it is also

dependent on the size, shape and quantity of shredded material in the hopper. There has been minimal investigation on the impact of extrusion temperature. What has been observed thus far is that at excessively high temperatures, ABS begins to exhibit deformities in the form of air bubbles leading to rougher filament that rips rather than stretches.

4.2 Design Verification

4.2.1 Hardware & Mechanical Verification

The validation of the hardware functionality was successfully done last term by assembling the board and verifying that it performs scans and outputs valid data.

The mechanical apparatus to house the system was verified by building it and ensuring everything fit together successfully. The successful build is shown in Figure 21. During assembly, it was determined that the base plate was not necessary, as the board was stable resting on a desktop on its standoffs. The centre of mass of the assembly was balanced even without the base plate. It is recommended that the base plate be included in assembly when the device is used in final application in a recycling line, to ensure no circuitry is exposed for safety and reliability reasons.

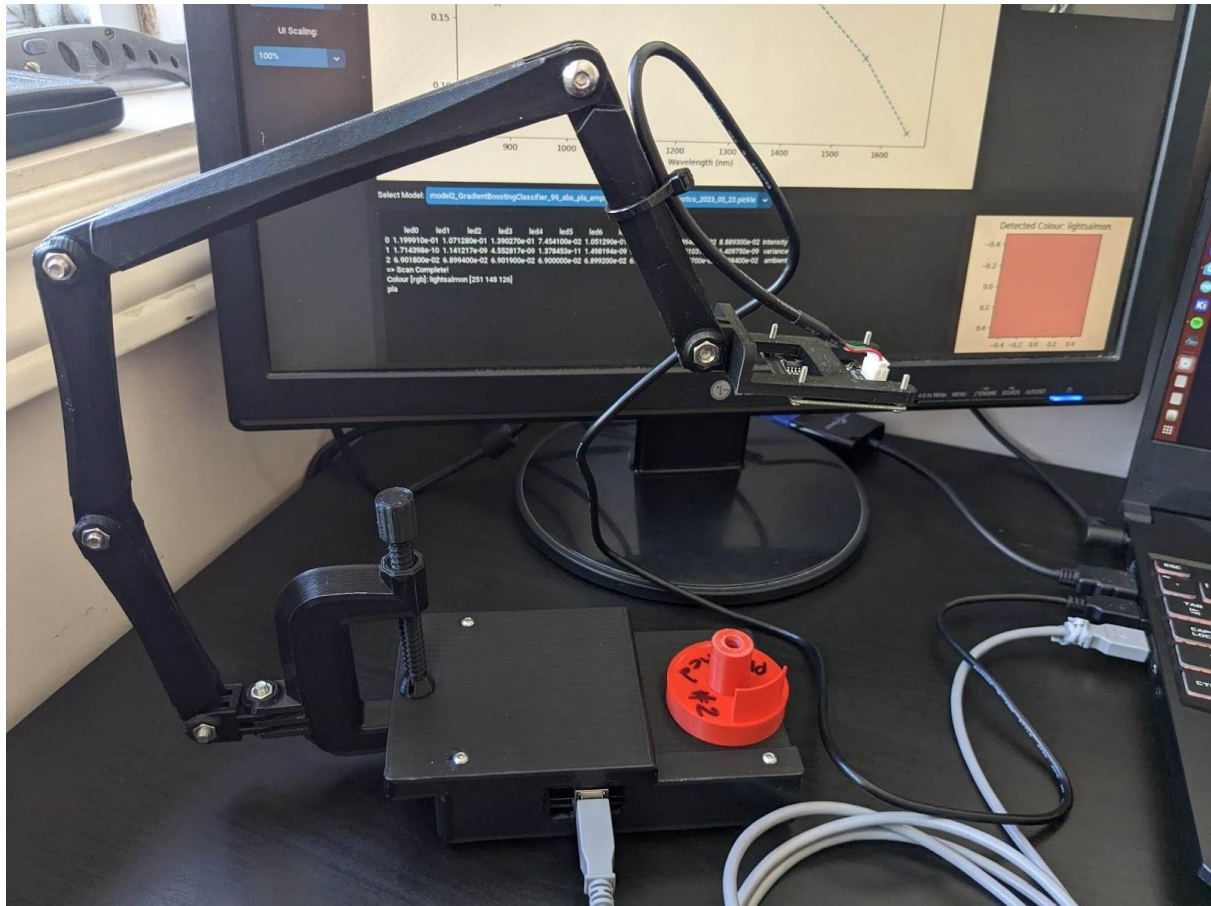


Figure 21. Assembled apparatus with the DNIR module in its cover and the camera on its mount.

4.2.2 Software Verification

There were a few different software systems to validate. In general, each system was tested and built individually, then all were merged into the end application which utilized each system. First was the firmware which as a first pass needed to compile, then flash the board successfully. The firmware had two different modes. It could be compiled to a Command Line Interface (CLI) mode which supported sending commands directly through a terminal and then performing actions. This mode was used to verify scan data for generation and was used for debugging. The other mode was a Serial mode where the board listened for serial data and parsed the incoming data to determine what command to execute. This was the default mode of operation.

Once incoming data from the board were verified, a data collection script and interface were created to send commands to the board to return data as either a single reading or as batches. The script saved the data locally in csv format. Further, the colour backend continuously pulled the live data feed from the camera, which could be easily displayed and visualized. Scripts were developed to test running the colour detection algorithm in real-time on the live feed.

All these components were merged in the end application which brought together the scan data feed, camera feed and colour detection, and the machine learning inference. Everything was combined in a GUI that was able to display the scan data in a plot along with the colour data and live camera feed. Additionally, output was provided to the user in the text box output area and the user was able to switch between different models to use for inference. This final product served as a final software verification step since each component was working together in a unified fashion and the interface provided direct feedback that allowed for validation.

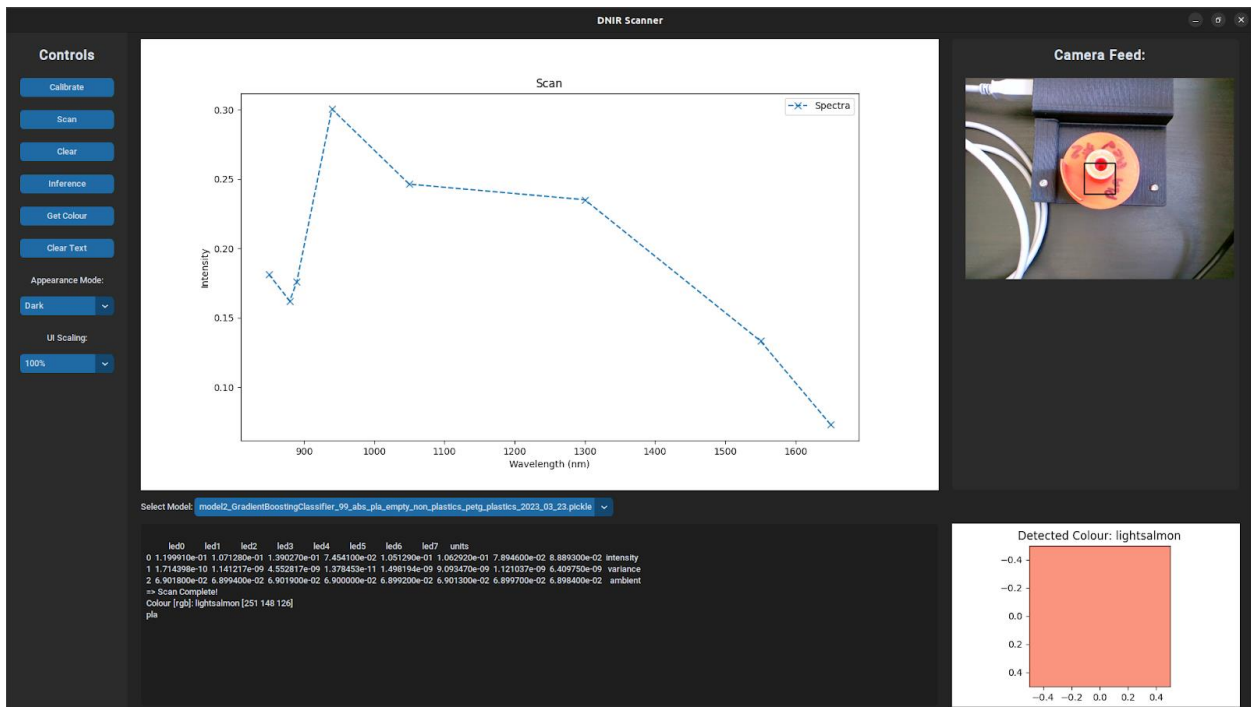


Figure 22. GUI Display showing camera feed, spectrum scan, inferred color, and inferred material.

4.2.3 Machine Learning Validation

Every training cycle, the data were split using an 80:20 training: validation split which randomly shuffled the data and allocated 80% of it to training and 20% to validation (Google, 2019). After the model is trained, the validation set is used to check the accuracy of the model on data it has never seen before. As part of the machine learning pipeline built, model metrics, hyperparameters and the output labels were saved to be used as reference and feedback on the next iteration of training, as seen in Figure 23. A small set of samples were reserved as the testing set for System verification. However, since the initial dataset of ~100 samples collected was relatively small, only a very small number of samples could be reserved for testing (Baheti, 2023).

```
1 {
2   "dataset": "./data/dataset3",
3   "labels": [
4     "abs",
5     "pla",
6     "empty",
7     "non_plastics",
8     "petg",
9     "plastics"
10  ],
11  "date": "2023_03_23",
12  "file": "model2_GradientBoostingClassifier_99_abs_pla_empty_non_plastics_petg_plastics_2023_03_23",
13  "id": 2,
14  "train-test-split": 0.2,
15  "score": 0.9915127309036446,
16  "args": "Namespace(verbose=False, save=True, optimize=False,
17           train=True, random_shuffle=False, check_overfitting=False, mock_data=True)",
18  "params": {
19    "ccp_alpha": 0.0,
20    "criterion": "friedman_mse",
21    "init": null,
22    "learning_rate": 1.0,
23    "loss": "log_loss",
24    "max_depth": 1,
25    "max_features": null,
26    "max_leaf_nodes": null,
27    "min_impurity_decrease": 0.0,
28    "min_samples_leaf": 1,
29    "min_samples_split": 2,
30    "min_weight_fraction_leaf": 0.0,
31    "n_estimators": 10,
32    "n_iter_no_change": null,
33    "random_state": 1,
34    "subsample": 1.0,
35    "tol": 0.0001,
36    "validation_fraction": 0.1,
37    "verbose": 0,
38    "warm_start": false
39  }
40 }
```

Figure 23. Model info captured during training. Includes validation accuracy, output labels, training parameters, and model hyperparameters.

Additional steps were taken to further validate the model. In general, two primary factors were considered: the accuracy of the model and how well it was generalized. For accuracy, the validation step reports a score as seen in Figure 23 above; however, an additional step is to generate a confusion matrix. A confusion matrix provides a visualization of false positives to negatives between the different output labels, indicating how and where each label is misclassified. You generally want to see all outputs on the diagonal. Further, since the dataset is balanced (each class

has the same proportion of data in the dataset), one class is not dominating the accuracy, but, if it were, it would be noticeable. Figure 24 below shows the confusion matrix for one of the trained models. Most of the classifications on the diagonal are true positives and approximately equal counts of data are in each.

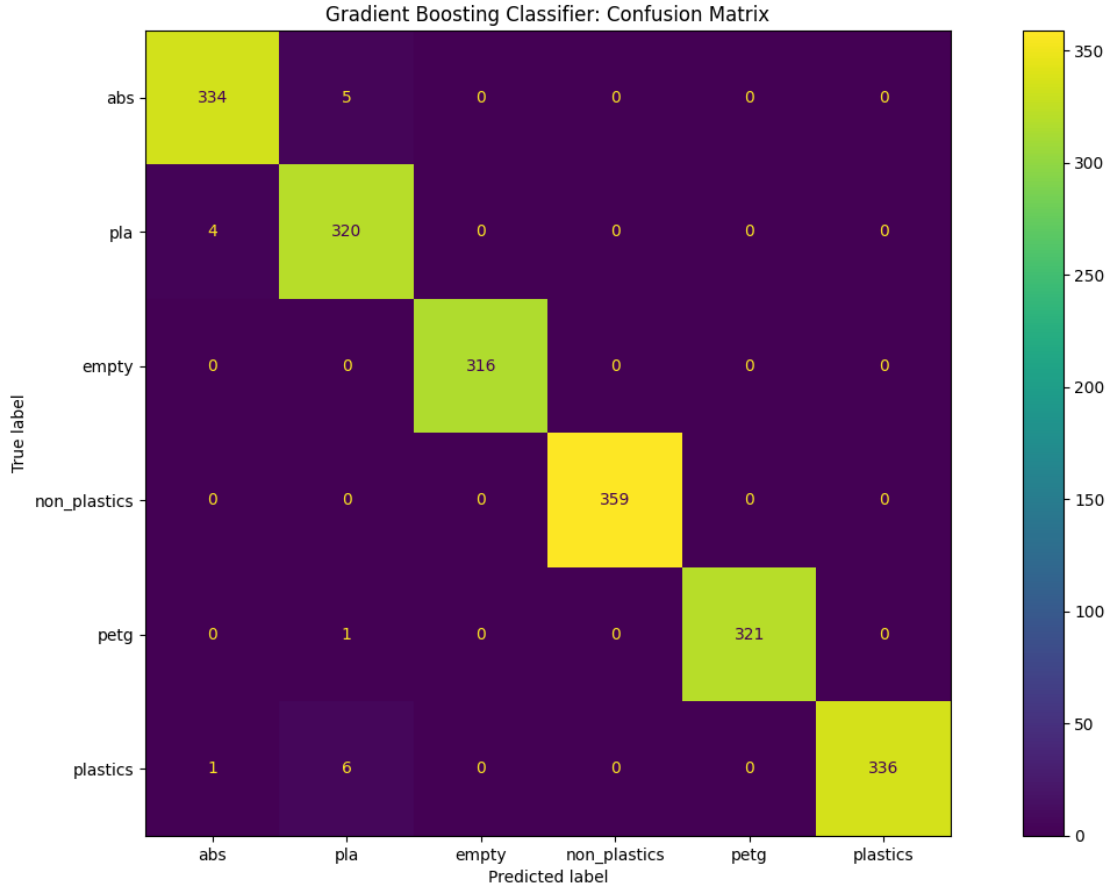


Figure 24. Confusion matrix of the gradient boosting classifier model for board v1.0 with the full set of trained labels: ABS, PLA, PETG, Empty, Plastics, and Non-Plastics.

The second notable metric is how well the model has been generalized. This ensures the model does not overfit (i.e., memorized) the data it was trained on. Therefore, once used on new data, there is a high confidence that the model will perform as expected. Apart from looking at the validation accuracy, the mean square error (MAE) of the training and testing data can be assessed (Google, 2019). The data are split into subsets, known as folds, the error from each fold is recorded for the training and test data. Figure 25 shows the mean square error for each fold. In general, it is desirable to have both these values below 0.3. Further, you want the gap between the mean square error of the training and validation (sometimes referred to as “test”) as close as possible. Low MAE for the training data and significantly higher for the validation data indicates that the model may be overfitting. In Figure 25, both sets are seen to be well below 0.3 MAE and, on average, the values between the training and validation differ significantly.

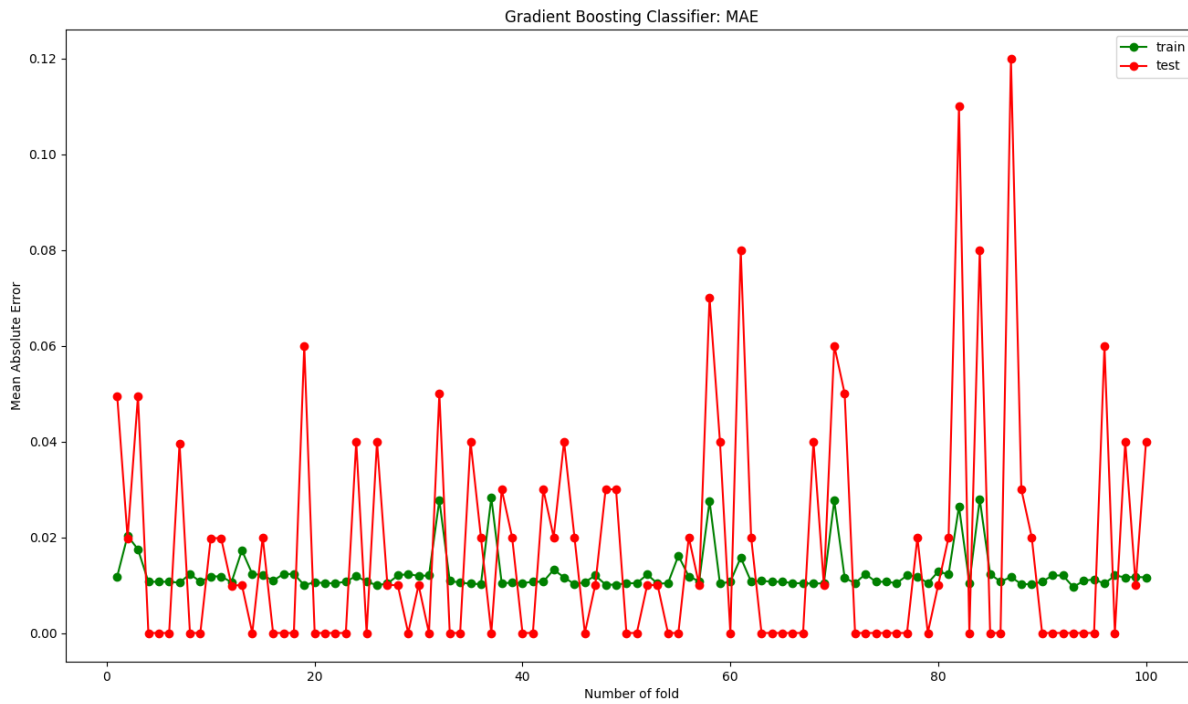


Figure 25. Mean square gradient boosting classifier model for board v1.0 with the full set of trained labels: ABS, PLA, PETG, Empty, Plastics, and Non-Plastics using k=100 folds.

4.2.4 System Verification

System verification began with simple operation, by assembling the apparatus, connecting the sensor and camera boards to the computer that was running the classification algorithms, and scanning a simple flat 3D-printed sample of waste. This ensured the system operated, and the software was receiving valid data from the hardware. Data verified included the reflectance of each of the eight wavelengths and the colour determination by the computer vision module, which was verified visually for accuracy.

The system was tested for robustness in a variety of different environments by repeatedly scanning diverse waste samples and checking for accuracy of classification. Tests were performed with around 15 samples in indirect sunlight, indirect sunlight and indirect lamp light, indirect lamp light at night, and direct overhead lamp light with indirect sunlight. In each scenario, indirect sunlight and direct or indirect lamp light, the test was done twice to test both domestic incandescent lighting and industrial fluorescent lighting. These situations were selected to simulate expected facility conditions in which the device may be used. Data from these verification tests were not recorded, as many of them were done implicitly during presentations at five different Capstone symposia, but the system performed consistently well in every situation except direct overhead fluorescent lamp light. The issue was resolved by shading the scanner area with a white scarf. Sometimes with direct overhead lighting, a glare would interfere with the colour readings, but this could be resolved by

holding up a hand to block the glare during the <1 second needed for the camera to get the colour of the sample.

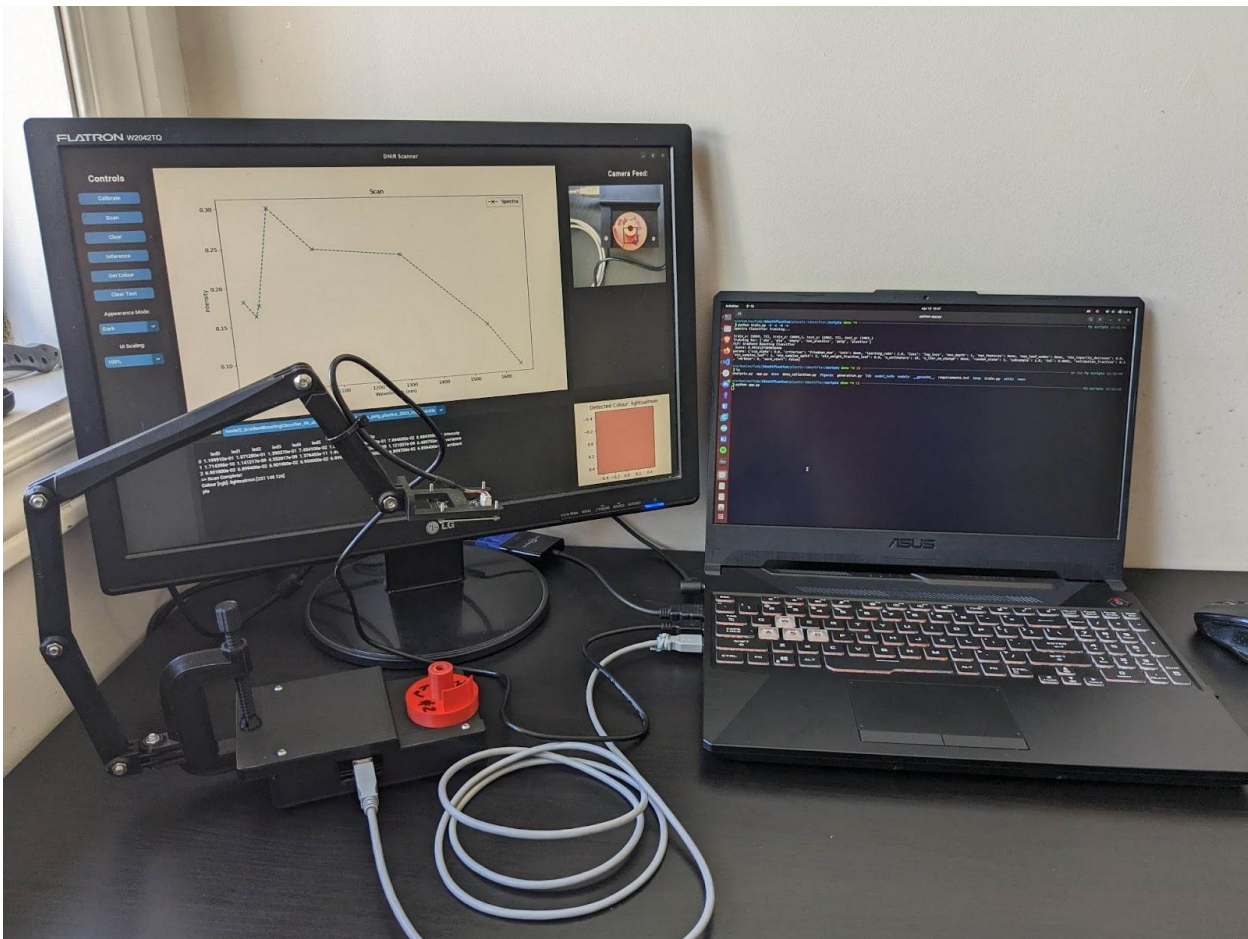


Figure 26. Complete system setup, with Apparatus and DNIR module connected to a host PC running the GUI application.

Table 8. Verification Results of Engineering Design Specification

Parameter	Relation	Value	Unit	Verification Method	Result
Primary Specifications					
Differentiate between PLA, ABS, and “other”				Demo	Pass
Reliable	within	95	%	Demo, testing	Pass (> 97%)

Functional Specifications					
Reject non-plastic materials	is	True/False		Demo, testing	Pass
Sense colour	within	+/- 10	nm	Demo, testing	Pass
Identification rate	≥	0.15	kg/h	Demo, testing	Pass (3 kg/h)*
Accept material of appropriate size	<	9 x 10.5 x 15	cm	Demo	Pass
Accessibility Specifications					
Cost	within	\$4.4 (PLA) \$3.44 (ABS)	CAD/kg	Analysis	Pass (\$0.81 – PLA) (\$1.31 – ABS)
Components available off-the-shelf or open-source				Analysis	Pass
Sustainability Specifications					
Energy demand	<	47.2 (PLA) 98.3 (ABS)	MJ/kg	Analysis	Pass (6.23 – PLA) (11.28 – ABS)
CO ₂ production	<	2.4 (PLA) 3.77 (ABS)	kg/kg	Analysis	Pass (1.16 – PLA) (1.66 – ABS)
Conform to <i>Restrictions on the Use of Certain Hazardous Substances (RoHS)</i> in electronic devices to prevent environmental contamination.			Analysis	Pass	
Creates minimal byproduct waste			Demo	Pass	

Safety Specifications					
Voltage in any part of device	<	50	V	Analysis, demo, testing	Pass (V < 5V)
Does not contain lead, mercury, cadmium, hexavalent chromium, poly-brominated biphenyls or polybrominated diphenyl ethers except as permitted in the Annex of Directive 2002/95/EC2 for certain lead solders			Inspection	Pass	
No exposed sharp edges or pinch points			Inspection, demo	Pass	
Does not emit fumes			Demo	Pass	
Conform to regulations of: International Electrotechnical Commission - (electrical device regulations) Directive 2002/95/EC - (Hazardous materials including heavy metals)			Demo	Pass	

*Identification rate based on a scan time of 6 seconds and average sample mass of 5 grams.

5.0 Safety, Regulations and Sustainability

5.1 Design for Safety

Research on 3D printer plastic brought to light the concern over the large amount of volatile organic compounds (VOCs) that are released during the melting of 3D printer filament. ABS has higher levels although it is a concern for PLA as well. Given that our design is an optical sensor that uses light but no heat, the concern over the release of fumes from plastic identification was eliminated. However, this brings up the safety concern of the potential for emitted lights to be harmful for human eyes. However, this was addressed by choosing LEDs that emit light close to the visible range and by using LEDs instead of LASERs.

Electrical safety was also addressed. The United States Department of Labour's *Occupational Health and Safety Association* specifies a maximum safe voltage of 50 V in their (OHSA, 2015). However, the plastic identification device we constructed has a voltage below 5 V, making it safe for users.

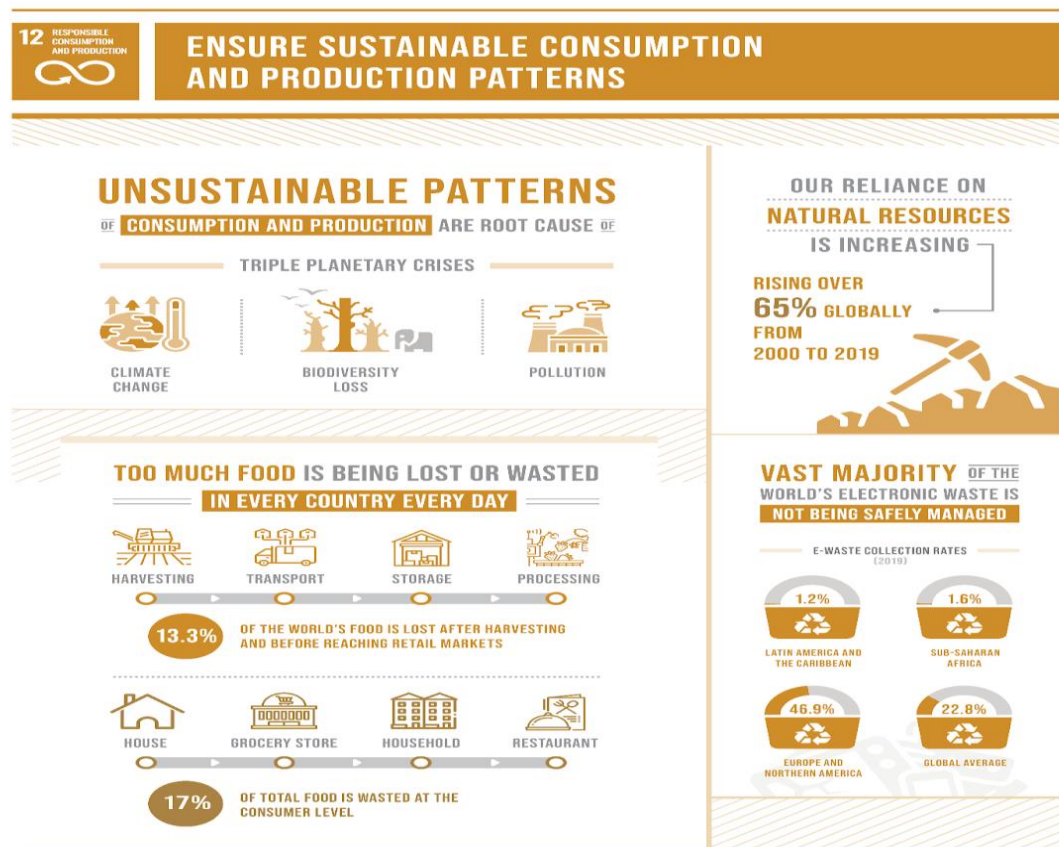
Finally, the device was constructed to be free of sharp edges and exposed circuitry, preventing cuts, electric shocks, fires and power surges (*Dangers Of Exposed Wiring!*, 2021).

5.2 Design for Regulatory Requirements

The constructed device meets all the relevant regulatory requirements. The International Electrotechnical Commission and the Occupational Health and Safety Association specify a maximum safe voltage of 50 V. Our device has a voltage much lower of around 5 V (OHS, 2015). In the Directive 2002/95/EC, the European Parliament and the Council restrict the use of certain hazardous substances, including heavy metals, in electrical and electronic equipment (European Parliament and The Council, 2003). Our device does not contain any hazardous substances. Commercial regulations, such as the Ontario Electrical Safety Code and Ontario Regulation 438/07, as well as CAN/CSA C22.2 No. 61010-1-2012, fall outside the scope of our project making them non-applicable (DPE1 Final Report, 2022).

5.3 Design for Sustainability

The project directly addresses various sustainable development goals (SDGs). The first targeted SDG is #12: responsible consumption and production. An overview of SDG #12 is shown in Figure 27:



THE SUSTAINABLE DEVELOPMENT GOALS REPORT 2022: UNSTATS.UN.ORG/SDGS/REPORT/2022/

Figure 27. An overview of the part of SDG #12 that our project focuses on (United Nations, n.d.)

This project focuses on target 12.2: “By 2030, achieve the sustainable management and efficient use of natural resources”, target 12.5: “By 2030, substantially reduce waste generation through prevention, reduction, recycling and reuse”, and target 12.7: “Promote public procurement practices that are sustainable, in accordance with national policies and priorities” (United Nations, n.d.).

This project also targets SDG #13: Climate Action. Industries are responsible for high amounts of carbon emissions which are contributing to climate change. Through recycling 3D printer filament, we are reducing the need for the extraction of virgin petroleum to produce ABS and the growing of corn for PLA. This greatly reduces the emissions from the production of 3D printer filament as will be discussed in section 5.4.

5.4 Assessment of Impact of the Engineering Design on Society and the Environment

Using available data on extraction and transportation from the Granta Edupack software (Ansys 2022), the carbon dioxide emissions were calculated for the current production of virgin PLA and ABS, and for the production of recycled filament. Similarly, the cost of producing virgin filament and that for recycled filament was calculated for PLA and ABS. These are shown in Figures 28 and 29.

To perform an analysis on the energy, cost, and emissions of the process, a combination of embodied energy, production, and transportation. The embodied energy, provided by Granta Edupack, can be thought of as the energy within the material that must be overcome for recycling.

Table 9. Embodied Energy of Recycling (Ansys 2022)

ABS	34.3 MJ/kg
PLA	16.1 MJ/kg

For production, the specification for average energy consumption and speed of shredding, extrusion and spooling provided by Felfil were used and the total energy was normalized on a 1 kg basis. Since embodied energy includes primary and secondary shredding, these estimates are conservative.

Table 10. Speed and Energy Consumption of Felfil Machines (Felfil 2022)

Operation	Speed	Average Energy Consumption	Total Energy
Shredder	4.00 kg/h	625 W	156.25 Wh
Extruder	0.15 kg/h	180 W	1200 Wh
Spooler	0.15 kg/h	60 W	400 Wh

The summation of all operations as well as the embodied energy of recycling provides an estimation of the total energy.

For transportation, four 3D printing makerspaces were located on Google maps, their distance from Velocity labs at the university of Waterloo was noted, and it was assumed that the van did not reach capacity until completing all roundtrips to each makerspace. This means the van was assumed to travel from Velocity to the makerspace and back to Velocity, which counted as one round trip. After, having done round trips between Velocity and each makerspace, a volume equivalent to one van load had been collected. This was done as a conservative estimate, although it would be much more efficient to do a single trip. Calculations were performed based on the Ford Transit Connect cargo van (*Momentum IoT* 2020) with a volume of 0.566 m³, fuel economy of 10.6 km/L, emission factor of 0.307 kg CO₂/km, and assuming gas cost of \$1.51/L. Based on the average density of plastic waste, the mass of waste collected was calculated to find the cost and emissions of transportation on a per kg basis.

To determine the total cost of the project, the total energy was multiplied by the on-peak Ontario energy cost (*Ontario Energy Board* n.d.) as a conservative estimate and added to the transportation cost. Similarly, for CO₂ emissions, the total energy was multiplied by the emission factor of Ontario (Canada 2022) to determine the CO₂ from grid electricity which was then added to the emissions from transportation. It should be noted that estimates do not include labor costs and any pre-sorting or cleaning was not considered.

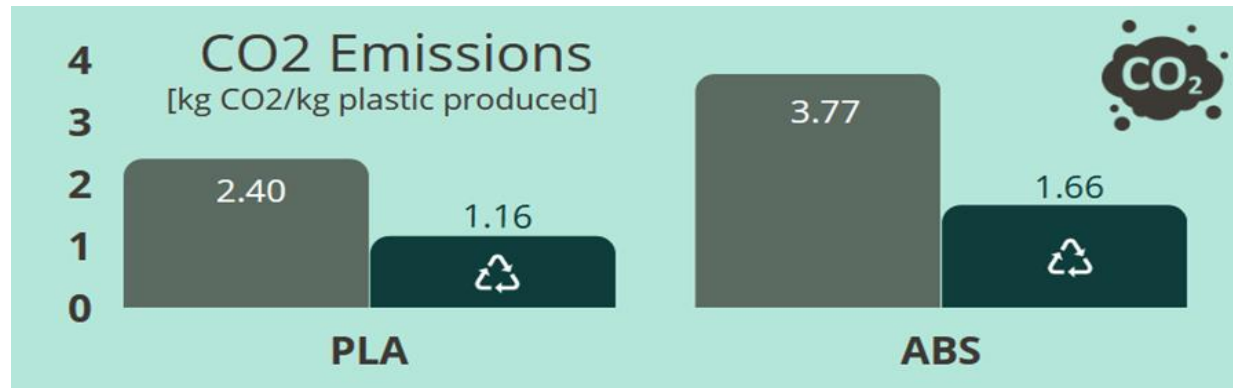


Figure 28. Reduced carbon dioxide emissions from recycling 3D printer filament.

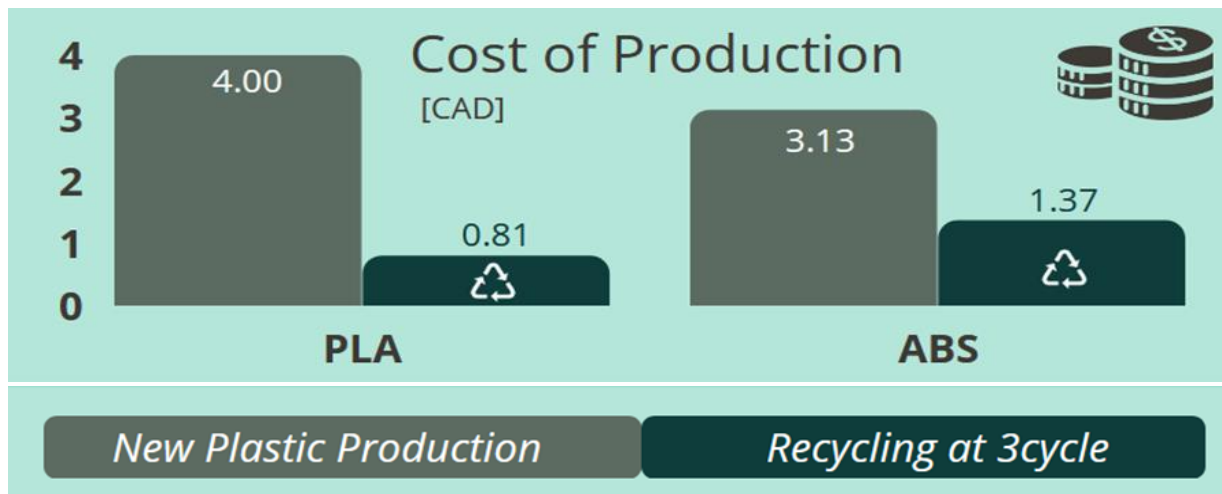


Figure 29. Reduced cost of production from recycling 3D printer filament.

As shown in Figure 28, recycling 3D printer filament produces about half of the carbon emissions than producing virgin filament. Similarly, as shown in Figure 29, there are considerable cost savings to producing recycled filament. The cost for producing recycled PLA is about 25% of that for virgin PLA and for recycled ABS, it is 44% of virgin ABS.

6.0 Project Management

6.1 Timeline & Schedule

The timeline for this project mostly conformed to schedule and planned contingency. As seen in Fig.6.1.1, the only task which was completed after planned contingency time was measuring the mechanical properties of contaminated recycled samples. This was because of delays getting 3cycle's recycling line set up and functioning, as the shredder, extruder, and spooler sourced from Felfil (*Felfil 2022*) required some repairs out of the box as well as a lot of trial and error to get the extruder and spooler to work together at the same pace. Resultantly, recycled filament of a consistent enough diameter to be suitable to feed into a 3D printer could not be produced until March, so the dog bone testing on the mechanical properties of the contaminated recycled sample could not be completed until late March. Ultimately, this investigation was not critical to the primary function of the project, and further investigation into allowable levels of contamination is recommended as future work.

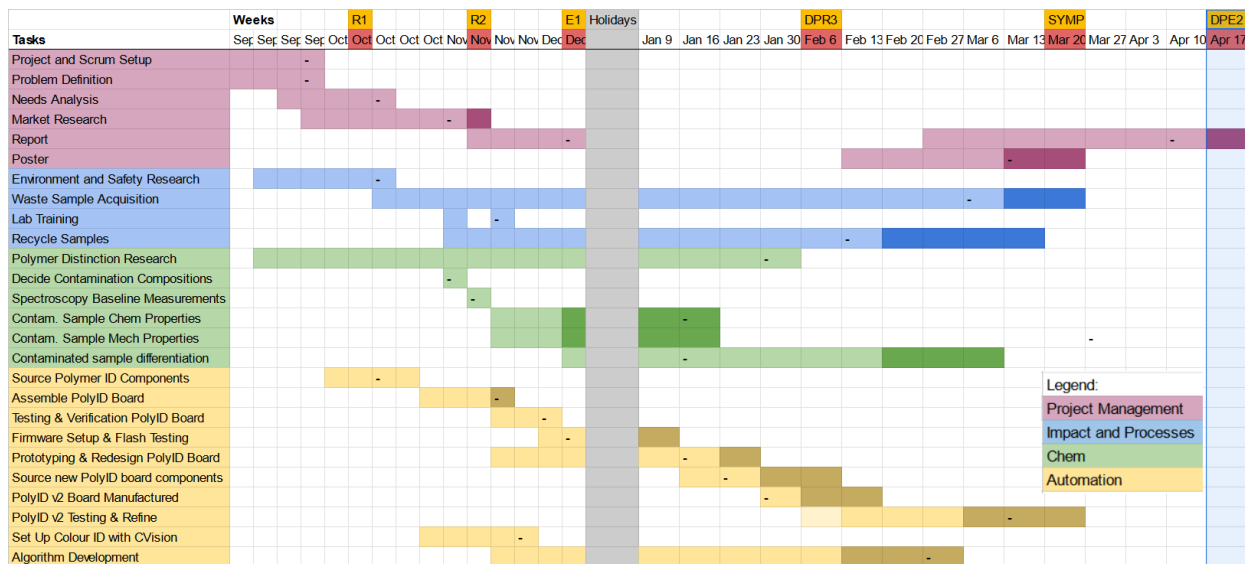


Figure 30. The planned schedule for the project represented as coloured cells with dark shades representing planned contingency, and dashes indicating when each task was completed in the timeline. Only one task was completed after planned contingency.

6.2 Lessons Learned

Working in an interdisciplinary team was highly valuable, not only because each team member brings diverse background knowledge and talent, but because involvement in different disciplines revealed opportunities for collaboration, mentorship, funding, and manufacturing which otherwise would have been missed. Collaborating with a student startup was also critical to the success of this project, because in addition to an even more diverse sample of disciplines, the project was well-funded and had a clearly defined scope relating to a very real need in the community.

Aggressively narrowing the project scope at the beginning of the project after doing an in-depth needs analysis created the space for the team to output a high quality of work and focus on continuous goals without needing to drop work part way through progress in the theoretical case where it is determined too late that the scope is too large for the timeline.

By finding an open-source project working in a similar application as the refined scope (*Plastic Scanner* 2023), the team saved months designing the circuit board and was able to use that time to test and refine the design as well as run laboratory experiments and help 3cycle establish a functional recycling line. This enforced the value of using resources conscientiously, so as not to “reinvent the wheel.”

Outsourcing the circuit board assembly saved initial build time and created very high-quality solder joints, but cost time and progress later when the manufacturer had reversed a few diodes, causing mysterious problems which were identified and corrected by the team. Providing clearer assembly documents when working with external manufacturers could reduce this type of setback in future projects.

When designing a system, it is important not to over trust the performance of any piece in the system, and to incorporate redundancy in design in case a piece does not perform as well as it should. This was learned from the mechanical apparatus, where despite including a calibration procedure in the software which was theoretically expected to compensate for any interference issues from the PLA reflectance, the cover and collar enclosure still caused an increase in false positives of PLA identification.

Even if equipment is purchased, such as the Felfil extruder and spooler, and is supposed to be ready to be used, it can take a considerable amount of time to learn how to use it. It is useful not to heavily rely on the fact that purchased equipment will work as intended. Allotting time for learning and troubleshooting can also ensure the project does not fall behind schedule.

7.0 Conclusions & Recommendations

7.1 Conclusions

The optical identification method of discrete near-infrared spectroscopy using a machine learning approach supplemented with computer vision colour detection proved effective. A diverse variety of samples of different materials and colours were identified successfully and subsequently recycled. The validation accuracy achieved was desirable and meets the specifications.

Furthermore, the system level verification overall achieved the end goal of identifying different 3D printed plastic types, along with being able to distinguish other non-suitable material in a timely manner and accuracy. Additionally, a deeper understanding of the material properties throughout the recycling process was gained. It was found that recycled PLA had a 40% reduction in tensile strength after one cycle of recycling. This does not discredit the motivation of recycling PLA, but rather provides an understanding of what applications it should be considered for. Further, after recycling, some characteristic peaks of ABS were not present, however they were mostly unchanged for PLA. Therefore, evidence suggests that it is possible to detect recycled ABS from a batch of samples using FTIR spectroscopy. Overall, the project was successful at developing a device to differentiate between the 3D-printed plastic types and developed a better understanding of the chemistry and material changes from recycling.

7.2 Recommendations

The 3cycle engineering capstone team provides the following recommendations:

Mechanical:

1. Make the collar for the DNIR board diodes out of a non-plastic material.
2. Add an overhead shade to block out direct lamp light, which sometimes interferes with NIR spectrum scanning and colour detection.
3. Make the DNIR cover/enclosure out of material that will not interfere with samples – either out of metal or a composite that is very different from 3D printed plastics.

Hardware:

1. Add a white LED next to the camera to shine on the piece when ambient lighting is dark to get the true colour.
2. Re-design board to use more than 8 NIR LEDs for a more precise spectrum for differentiating more reliably between many materials.

Firmware:

1. Disable the automatic colour-adjustment of the camera module which sometimes washes out bright colours.
2. Do more research into which wavelengths in the NIR range are best for differentiating 3D-printed plastics, since our preliminary FTIR data did not measure reflectance below 2500 nm (wavenumber 4000 cm^{-1}).
3. Optimize the serial backend for sending data between the DNIR board and the host computer to make the scans much faster.

Software:

1. Integrate a database for storing scan data, model info and other data, either hosted locally or in the cloud.
2. Dockerize and/or create a binary/executable of the GUI application so it can be set up and deployed on any system more easily.
3. Optimize the serial backend interface, in conjunction with Firmware recommendation #3 above.

Machine Learning & Algorithms:

1. Try training a model on contaminated samples and measure the reliability of identification. This can help with Experiment recommendation #1 below.
2. Train a model on stringy failed prints and measure the reliability of identification, to inform the capabilities of the system.
3. Integrate tools such as MLFlow to better track trained models and model info during training pipeline.
4. Collect more waste samples to generate a much larger dataset to train the model on.
5. Explore more deep learning models and architectures.

Experiments:

1. We know contamination can be detected with continuous FTIR spectroscopy, but can contamination be detected in the NIR range with discrete spectroscopy?
2. How much contamination is acceptable in a print made of recycled filament? At what point does it affect extrusion or strength too much to be permissible?
3. How many recycling cycles can be performed with ABS and PLA before the properties degrade too much?

7.3 Acknowledgements

We greatly appreciate the help we received on this project from numerous people. We would like to thank Professor Tizazu Mekonnen for his role as capstone advisor. We appreciate his guidance, recommendations regarding the chemical experiment portion of this project, and the use of his

laboratory equipment. We would like to thank Binh Minh Trinh for supporting our use of equipment in the Mekonnen Lab. We would like to thank Professor Simar Saini for sharing his knowledge on spectrometry and spectroscopy, and for helping us take some NIR spectrometry readings using his equipment to inform our design. We appreciate the instruction, support, and guidance from Professor Oscar Nespoli throughout GENE 403 and 404.

This project would not have been possible without the support of Jason Amri and the 3cycle team, the funding from the University of Waterloo's Sustainability Office, and the open-source board from the PlasticScanner development community. We would also like to thank Jeff and Accelerated Systems Inc. for helping manufacture our project free of charge.

References

Abayazeed, M., Baribeau, J., Fraser Semenoff, M., and Pistek, U. (2022, December 13). *Design Project Report 1*.

<https://drive.google.com/file/d/15FZkQvQh5yp94oCfIyQQXDCKPnHCOtYf/view?usp=sharing>

Amri, J. (2022, March 7). 3cycle - The 3D Printing Waste Problem [Video].

<https://drive.google.com/file/d/15ZhEkKFbYGmmIjhP9ZkYl0tdx6pQwpUY/view>

Ansys, Granta Edupack 2022 R1, Release 22.1.2. ANSYS Inc.

Baheti, P. (2023, March 2). Train test validation split: How to & best practices [2023]. V7. Retrieved April 18, 2023, from <https://www.v7labs.com/blog/train-validation-test-set>

Canada, E. and C. C. (2022, June 8). Government of Canada. Canada.ca. Retrieved April 17, 2023, from <https://www.canada.ca/en/environment-climate-change/services/climate-change/pricing-pollution-how-it-will-work/output-based-pricing-system/federal-greenhouse-gas-offset-system/emission-factors-reference-values.html>

Digi-key Electronics. (n.d.). Retrieved January 22, 2023, from <https://www.digikey.ca/>

Electricity rates. Electricity rates | Ontario Energy Board. (n.d.). Retrieved April 17, 2023, from <https://www.oeb.ca/consumer-information-and-protection/electricity-rates>

European Commission. (n.d.). Waste from Electrical and Electronic Equipment (WEEE). Retrieved December 10, 2022, from https://environment.ec.europa.eu/topics/waste-and-recycling/waste-electrical-and-electronic-equipment-weee_en

European Parliament and The Council. (2003, 27 January). *DIRECTIVE 2002/95/EC*.
https://dtsc.ca.gov/wp-content/uploads/sites/31/2021/02/2002_95_EC ADA.pdf

FELFIL filament maker: Make your own 3D printing filament with Felfil Evo. Felfil. (2022, September 28). Retrieved April 17, 2023, from <https://felfil.com/?v=5ea34fa833a1>

Feature Vector | Brilliant Math & Science Wiki. (n.d.). Brilliant.org.

<https://brilliant.org/wiki/feature-vector/>

Google. (2022, July 18). Training and test sets: Splitting data | machine learning | google developers. Google. Retrieved April 18, 2023, from <https://developers.google.com/machine-learning/crash-course/training-and-test-sets/splitting-data>

Google. (2019). Training and Test Sets: Splitting Data | Machine Learning Crash Course. Google Developers. <https://developers.google.com/machine-learning/crash-course/training-and-test-sets/splitting-data>

HeyVye. (2020, October 10). Modular Mounting System Update. UltiMaker Thingiverse. Retrieved April 17, 2023, from <https://www.thingiverse.com/thing:4619937>

Momentum IoT. *What is the most fuel-efficient cargo van?* (2020, September 11). Retrieved April 17, 2023, from <https://momentumiot.com/what-is-the-most-fuel-efficient-cargo-van/>

OHSA. (2015). Guarding requirements for 50 volts or more DC. (n.d.). United States Department of Labour. Retrieved December 11, 2022, from <https://www.osha.gov/laws-regulations/standardinterpretations/2015-09-04>

Plastic Scanner. Plastic Scanner. (2023, April 4). Retrieved April 17, 2023, from <https://plasticscanner.com/>

Straller, Armin & Gessler, Bernhard. (2019). Identification of Plastic Types Using Discrete Near Infrared Reflectance Spectroscopy.

The Local Electrician (2021, September 26). Dangers Of Exposed Wiring! <https://www.thelocalelectrician.com.au/dangers-of-exposed-wiring/>

Tiseo, I. (2022, February). Average cost to landfill municipal solid waste in the United States in 2020 and 2021, by region. Statista. Retrieved December 14, 2022, from <https://www.statista.com/statistics/692063/cost-to-landfill-municipal-solid-waste-by-us-region/>

United Nations. (n.d.). *Goal 12: Ensure Sustainable Consumption and Production Patterns*. United Nations: Department of Economic and Social Affairs. Retrieved April 14, 2023, from <https://sdgs.un.org/goals/goal12>

United Nations. (n.d.). *Goal 13: Take Urgent Action to Combat Climate Change and Its Impacts*. United Nations: Department of Economic and Social Affairs. Retrieved April 14, 2023, from <https://sdgs.un.org/goals/goal13>

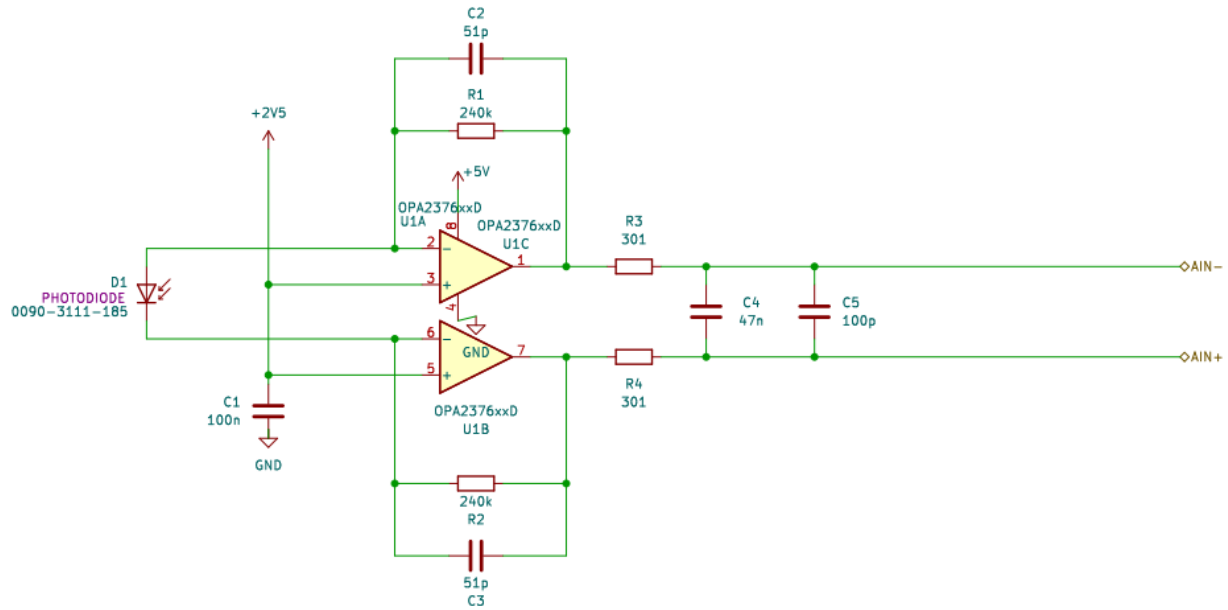
Appendix A

Design Solution Description and Engineering Data

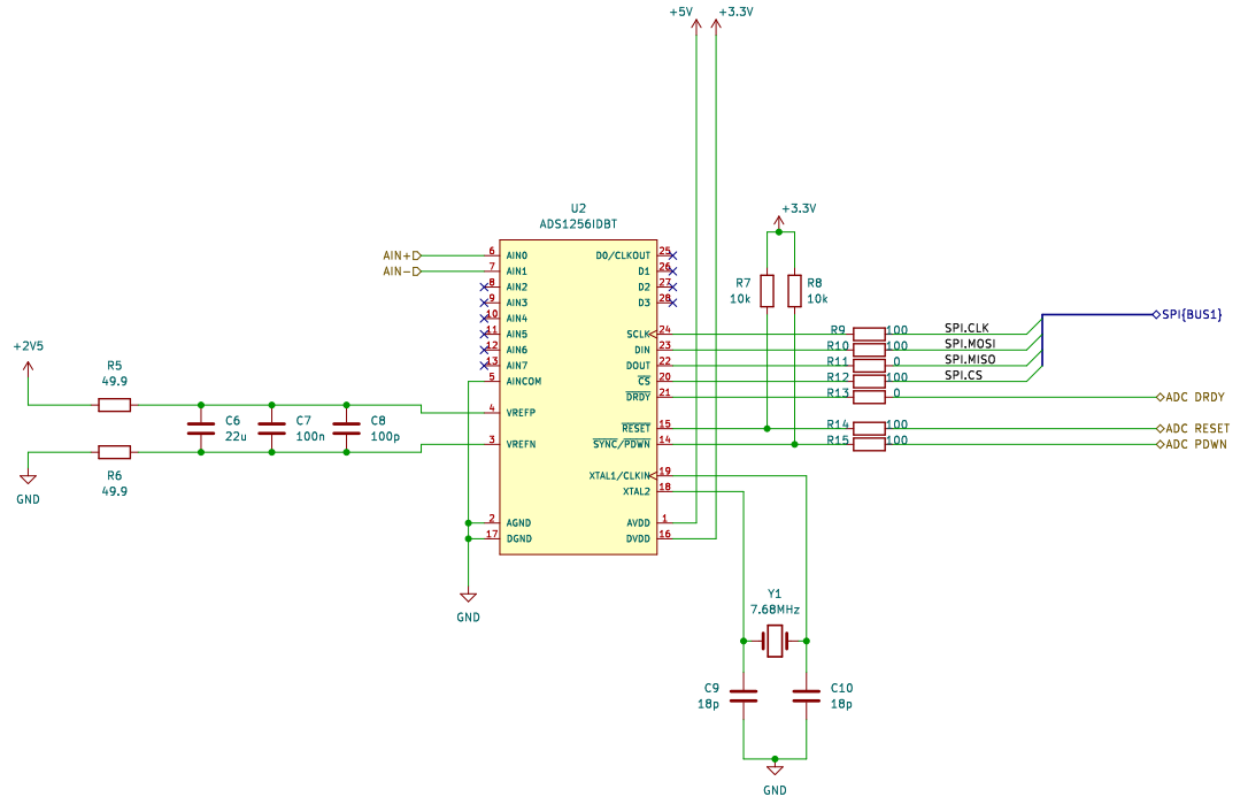
DNIR Board Schematics: 10-2022-DNIR Rev. 1

Team 10, 3cycle

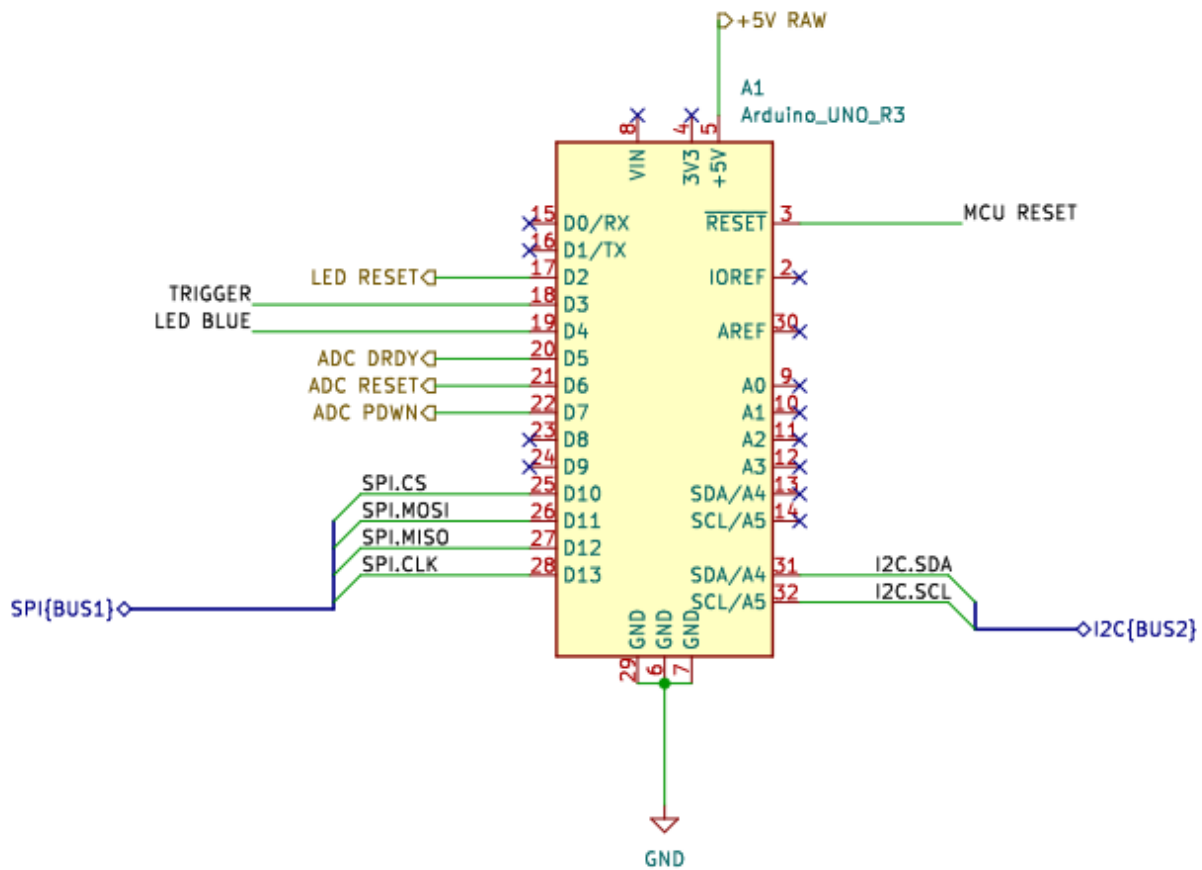
Sensor



ADC

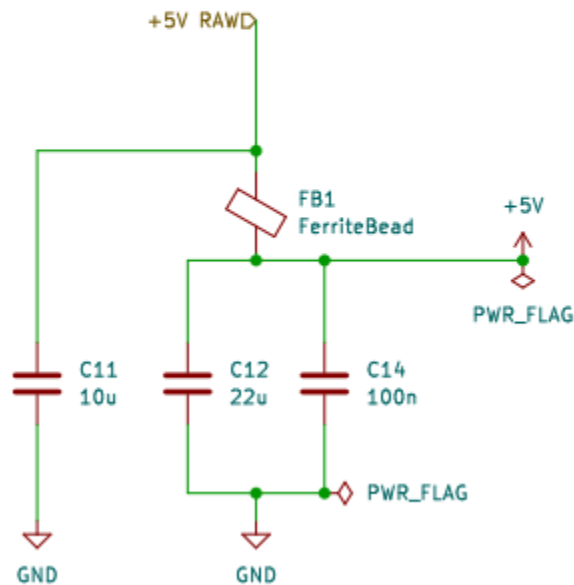


MCU

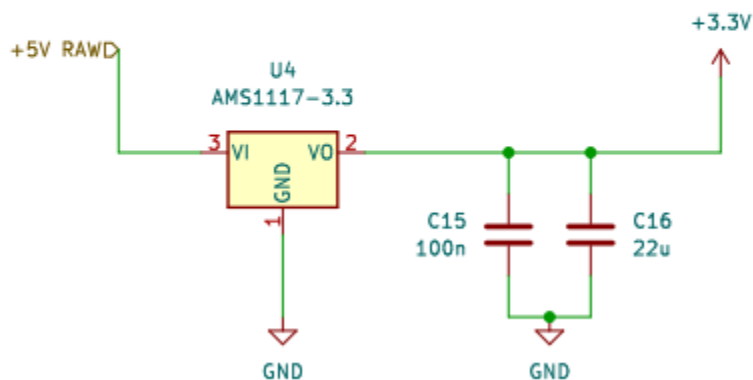


Power

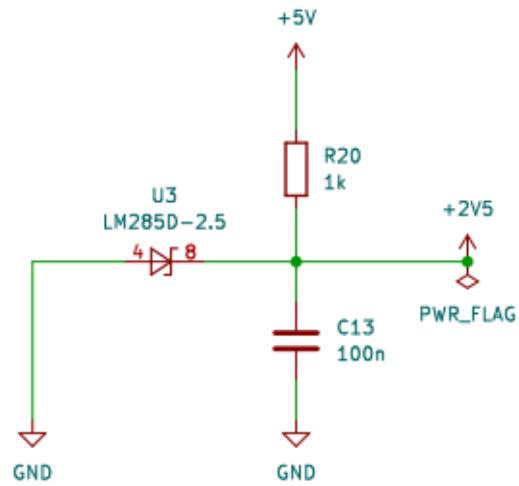
Main Power Supply +5V



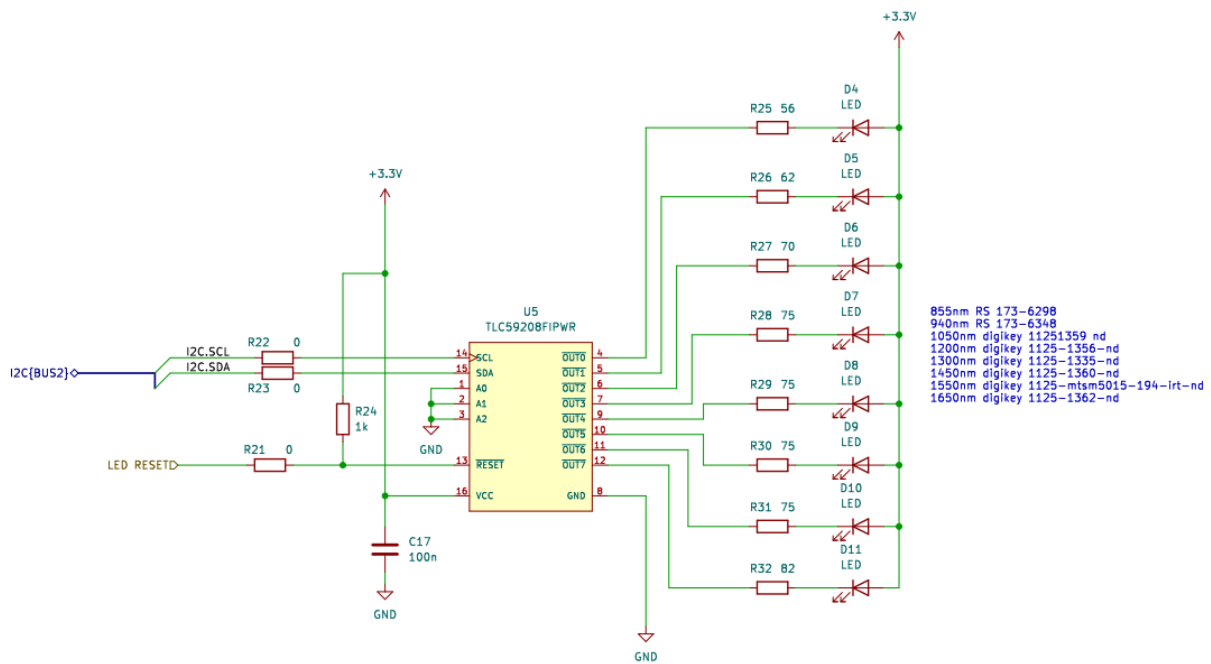
+3.3v



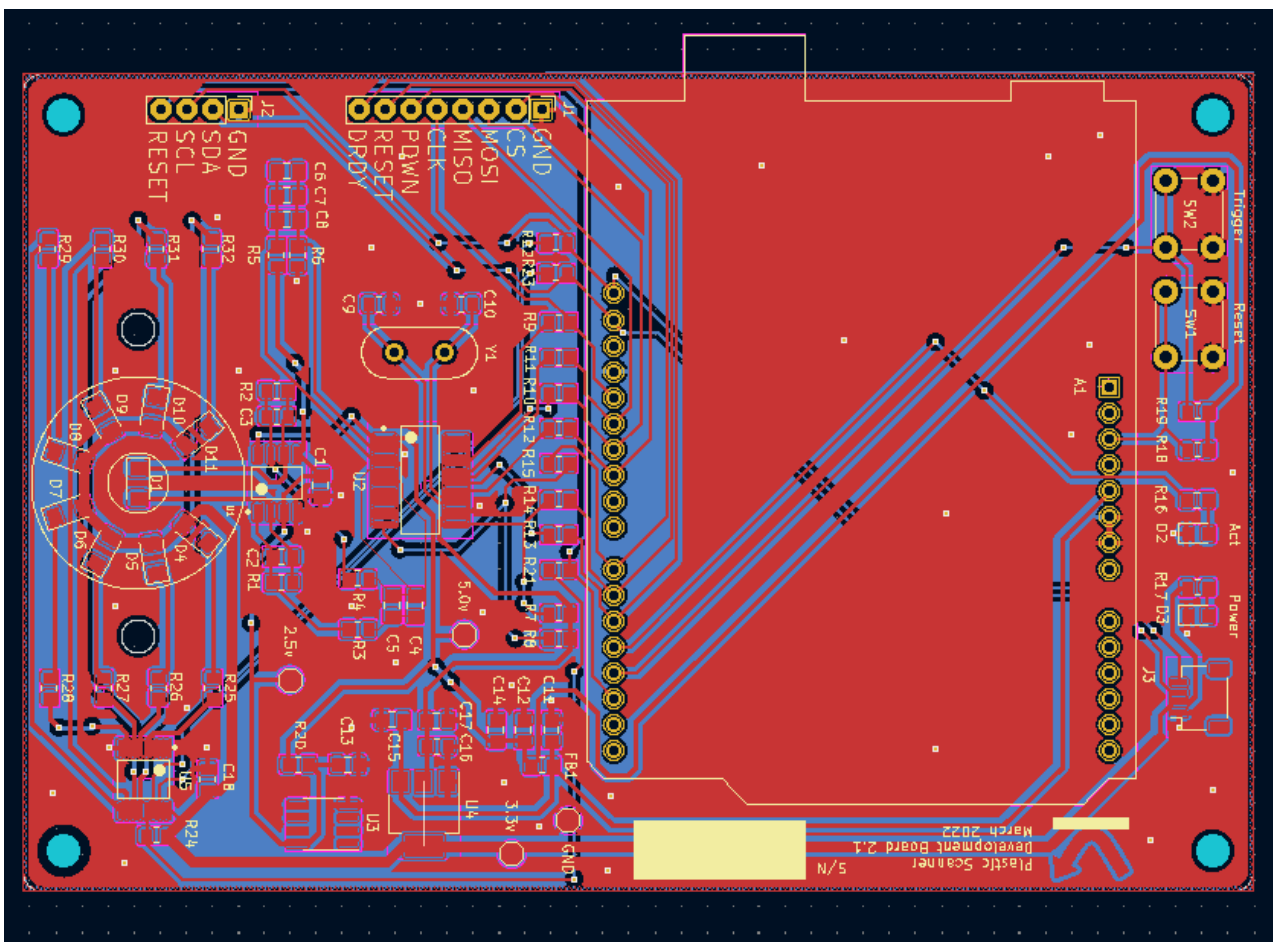
2.5v reference



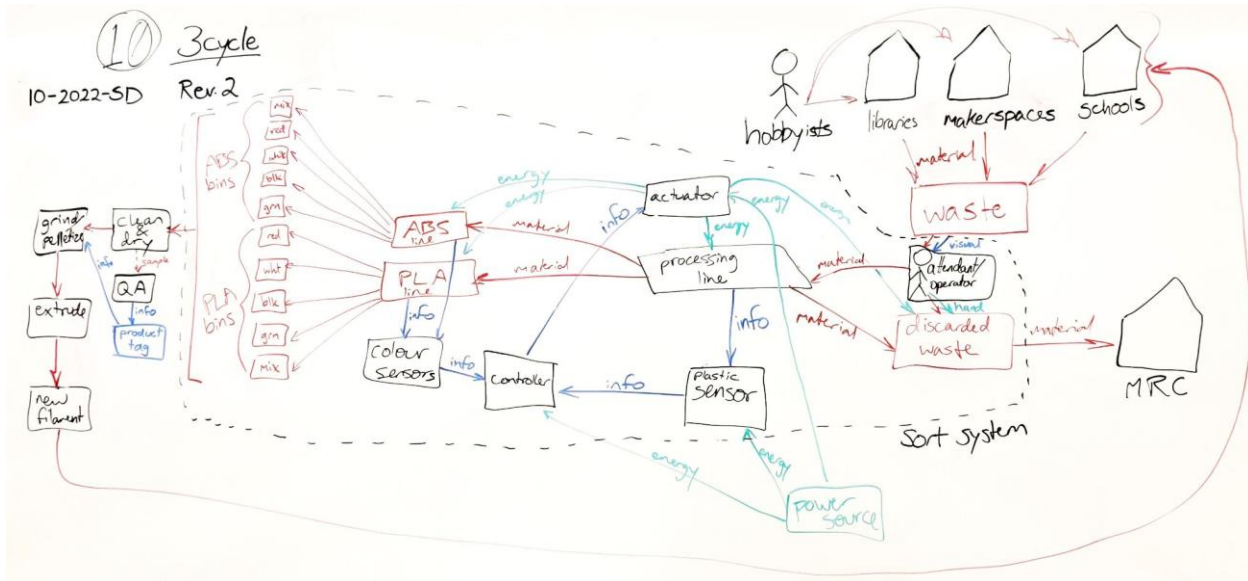
LED



DNIR Board Layout

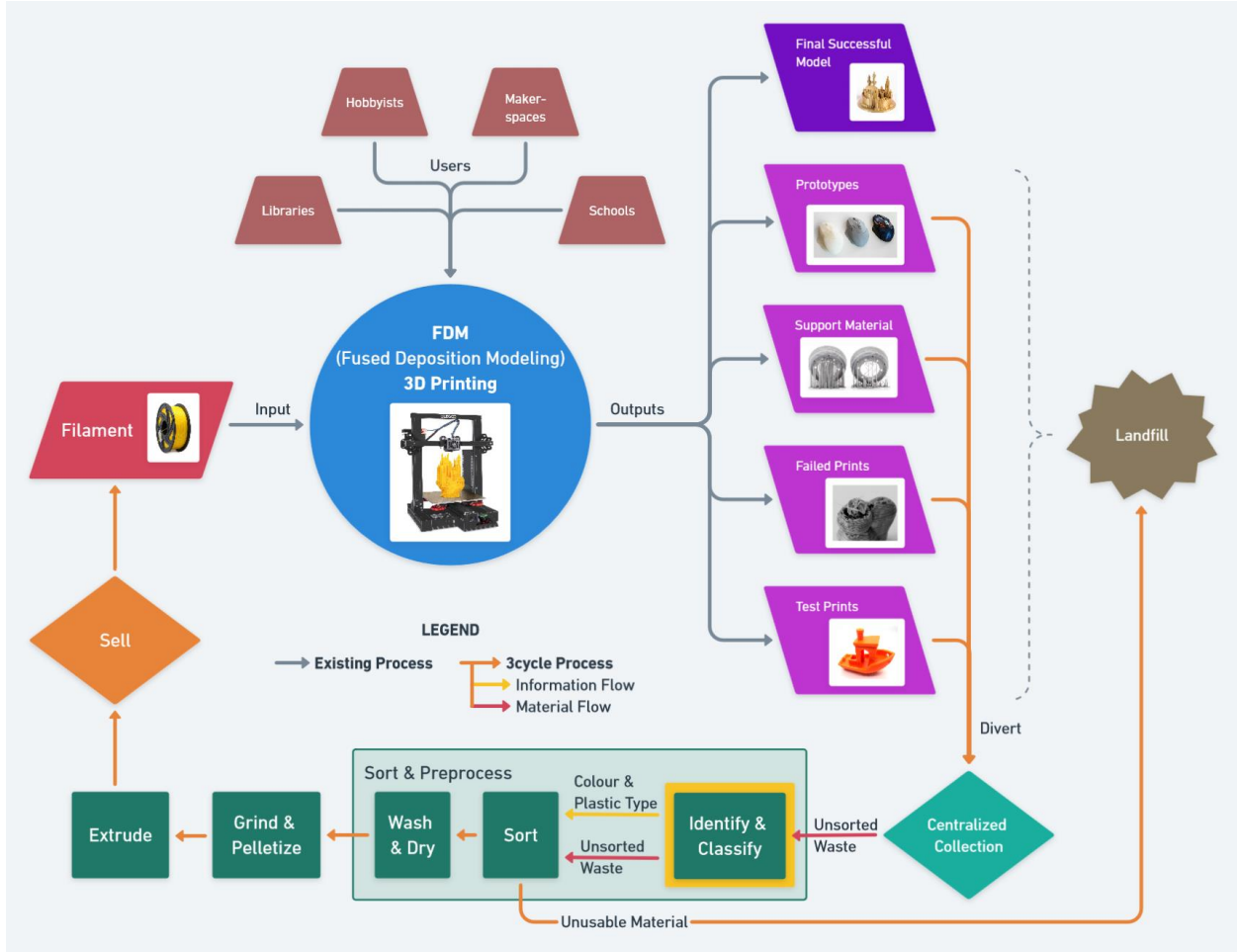


System Level Representation: 10-2022-SD Rev. 2



System Level Representation: 10-2022-SD Rev. 3

Team 10, 3cycle



Engineering Design Specifications: 10-2022-EDS Rev 1, Rev 2, Rev 3,
Rev 4

Code: GitHub.com/UrbanPistek/3dentification

The screenshot shows the GitHub repository page for 'UrbanPistek/3dentification'. The repository is public and has 29 commits in the last month. The code tab is selected, showing a list of files and their recent activity:

File	Description	Last Commit
plastic-cv	Model-development (#12)	last month
plastic-identifier	Model-development (#12)	last month
plastic-scanner	Automated data collection (#4)	4 months ago
rust	Inference-application (#11)	last month
utils	Added skeleton for system architecture with docker containers (#6)	4 months ago
.gitignore	Model-development (#12)	last month
CITATION.cff	Create CITATION.cff	4 months ago
Dockerfile	Added skeleton for system architecture with docker containers (#6)	4 months ago
LICENSE	Create LICENSE	6 months ago
README.md	Added skeleton for system architecture with docker containers (#6)	4 months ago
app.py	Added skeleton for system architecture with docker containers (#6)	4 months ago
docker-compose.yaml	Added skeleton for system architecture with docker containers (#6)	4 months ago

The repository has 0 stars, 3 watching, and 0 forks. It includes links for Readme, GPL-3.0 license, Cite this repository, Report repository, and Create a new release.

DNIR Module Parts List: 10-2022-BOM Rev 2

Team 10, 3cycle

Itm	Qty	Ref(s)	Value	LibPart	Footprint	Datasheet
1	1	A1	Arduino_UNO_R3	MCU_Module:Arduino_UNO_R3	Module:Arduino_UNO_R3	Source
2	6	C1, C7, C13, C14, C16, C18	100n	Device:C	Capacitor_SMD:C_0805_2012Metric_Pad1.18x1.45mm_HandSolder	Source
3	2	C2, C3	51p	Device:C	Capacitor_SMD:C_0805_2012Metric_Pad1.18x1.45mm_HandSolder	Source
4	1	C4	47n	Device:C	Capacitor_SMD:C_0805_2012Metric_Pad1.18x1.45mm_HandSolder	Source
5	2	C5, C8	100p	Device:C	Capacitor_SMD:C_0805_2012Metric_Pad1.18x1.45mm_HandSolder	Source
6	3	C6, C12, C17	22u	Device:C	Capacitor_SMD:C_0805_2012Metric_Pad1.18x1.45mm_HandSolder	Source
7	2	C9, C10	18p	Device:C	Capacitor_SMD:C_0805_2012Metric_Pad1.18x1.45mm_HandSolder	Source
8	2	C11, C15	10u	Device:C	Capacitor_SMD:C_0805_2012Metric_Pad1.18x1.45mm_HandSolder	Source
9	1	D1	730-1100nm (Peak @940nm)	Device:PhotoD	D_1206_3216Metric_Pad1.42x1.75mm_HandSolder	Source
10	1	D2	LED BLUE	Device:LED	LED_SMD:LED_0805_2012Metric_Pad1.15x1.40mm_HandSolder	Source
11	1	D3	LED RED	Device:LED	LED_SMD:LED_0805_2012Metric_Pad1.15x1.40mm_HandSolder	Source
12	1	D4	740 nm	Device:LED	LED_SMD:LED_1206_3216Metric_Pad1.42x1.75mm_HandSolder	Source
13	1	D5	850 nm	Device:LED	LED_SMD:LED_1206_3216Metric_Pad1.42x1.75mm_HandSolder	Source
14	1	D6	870 nm	Device:LED	LED_SMD:LED_1206_3216Metric_Pad1.42x1.75mm_HandSolder	Source
15	1	D7	880 nm	Device:LED	LED_SMD:LED_1206_3216Metric_Pad1.42x1.75mm_HandSolder	Source
16	1	D8	890 nm	Device:LED	LED_SMD:LED_1206_3216Metric_Pad1.42x1.75mm_HandSolder	Source

17	1	D9	940nm	Device:LED	LED_SMD:LED_1206_3216Metric_Pad1.42x1.75mm_HandSolder	Source
18	1	D10	980 nm	Device:LED	LED_SMD:LED_1206_3216Metric_Pad1.42x1.75mm_HandSolder	Source
19	1	D11	1050 nm	Device:LED	LED_SMD:LED_1206_3216Metric_Pad1.42x1.75mm_HandSolder	Source
20	1	FB1	FerriteBead	Device:FerriteBead	Resistor_SMD:R_0805_2012Metric_Pad1.20x1.40mm_HandSolder	Source
21	1	J1	ADC Debug	Connector_Generic:Conn_01x08	Connector_PinHeader_2.54mm:PinHeader_1x08_P2.54mm_Vertical	Urban
22	1	J2	LED Debug	Connector_Generic:Conn_01x04	Connector_PinHeader_2.54mm:PinHeader_1x04_P2.54mm_Vertical	Urban
23	1	J3	Qwiic	Connector_Generic:Conn_01x04	Connector_JST:JST_SH_SM04B-SRSS-TB_1x04-1MP_P1.00mm_Horizontal	Source
24	2	R1, R2	240k	Device:R	Resistor_SMD:R_0805_2012Metric_Pad1.20x1.40mm_HandSolder	Source
25	2	R3, R4	301	Device:R	Resistor_SMD:R_0805_2012Metric_Pad1.20x1.40mm_HandSolder	Source
26	2	R5, R6	49.9	Device:R	Resistor_SMD:R_0805_2012Metric_Pad1.20x1.40mm_HandSolder	Source
27	4	R7, R8, R18, R19	10k	Device:R	Resistor_SMD:R_0805_2012Metric_Pad1.20x1.40mm_HandSolder	Source
28	7	R9, R10, R12, R14, R15, R16, R17	100	Device:R	Resistor_SMD:R_0805_2012Metric_Pad1.20x1.40mm_HandSolder	Source
29	5	R11, R13, R21, R22, R23	0	Device:R	Resistor_SMD:R_0805_2012Metric_Pad1.20x1.40mm_HandSolder	Source
30	2	R20, R24	1k	Device:R	Resistor_SMD:R_0805_2012Metric_Pad1.20x1.40mm_HandSolder	Source
31	1	R25	52	Device:R	Resistor_SMD:R_0805_2012Metric_Pad1.20x1.40mm_HandSolder	Source

32	1	R26	200	Device:R	Resistor_SMD:R_0805_2012Metric_Pad1.20x1.40mm_HandSolder	Source
33	3	R27, R30, R31	150	Device:R	Resistor_SMD:R_0805_2012Metric_Pad1.20x1.40mm_HandSolder	Source
34	1	R28	220	Device:R	Resistor_SMD:R_0805_2012Metric_Pad1.20x1.40mm_HandSolder	Source
35	1	R29	240	Device:R	Resistor_SMD:R_0805_2012Metric_Pad1.20x1.40mm_HandSolder	Source
36	1	R32	40	Device:R	Resistor_SMD:R_0805_2012Metric_Pad1.20x1.40mm_HandSolder	Source
37	1	SW1	MCU_RESET	Switch:SW_Push	Button_Switch_THT:SW_PUSH_6mm	Urban
38	1	SW2	TRIGGER	Switch:SW_Push	Button_Switch_THT:SW_PUSH_6mm	Urban
39	1	U1	OPA2376xxD	Amplifier_Operational:OPA2376xxD	ee:Texas_Instruments-OPA2376AID-Level_A	Source
40	1	U2	ADS1256IDBT	ADS1256:ADS1256IDBT	ADS1256:Texas_Instruments-ADS1256IDBT-Level_A	Source
41	1	U3	LM285D-2.5	Reference_Voltage:LM285D-2.5	Package_SO:SOIC-8_3.9x4.9mm_P1.27mm	Source
42	1	U4	AMS1117-3.3	Regulator_Linear:AMS1117-3.3	Package_TO_SOT_SMD:SOT-223-3_TabPin2	Source
43	1	U5	TLC59208FIPWR	TLC59208:TLC59208FIPWR	TLC59208:Texas_Instruments-TLC59208FIPWR-Level_A	Source
44	1	Y1	7.68MHz	Device:Crystal	Crystal:Crystal_HC49-U_Vertical	Source

Appendix B

Verification and Validation Data

Polymer Experiment Data: 10-2023-PLOY Rev. 1

Team 10, 3cycle

Table B.1. Virgin PLA Samples

Sample Name	Thickness (mm)	Width (mm)	Gauge Length (mm)
PLA_1	3.27	6.35	22.00
PLA_2	3.19	6.31	22.00
PLA_3	3.22	6.18	22.00
PLA_4	3.12	6.43	22.00
PLA_5	3.16	6.20	22.00

Table B.2. Virgin PLA Mechanical Testing Results

Name	Young's Modulus	Ultimate Tensile Strength	Strain at Break	Time of Break
Unit	GPa	MPa	%	sec
PLA_1	0.66378	49.6944	11.1939	14.78
PLA_2	0.77898	53.0594	11.3994	15.05
PLA_3	0.74101	54.7045	15.1262	19.97
PLA_4	0.82304	49.8999	10.5202	13.89
PLA_5	0.67889	53.7916	11.1106	14.67
Average	0.73714	52.2300	11.8701	15.672
Standard Deviation	0.06693	2.29719	1.84933	2.44105
Range	0.15926	5.01010	4.60600	6.08

Table B.3. Recycled PLA Samples

Sample Name	Thickness (mm)	Width (mm)	Gauge Length (mm)
RPLA_1	3.30	6.27	22.00
RPLA_2	3.09	6.27	22.00

RPLA_3	3.07	6.03	22.00
RPLA_4	3.14	6.05	22.00
RPLA_5	3.07	6.05	22.00

Table B.4. Recycled PLA Mechanical Testing results

Name	Young's Modulus	Ultimate Tensile Strength	Strain at Break	Time of Break
Unit	GPa	MPa	%	sec
RPLA_1	0.87650	56.3604	12.9146	17.05
RPLA_2	1.29030	57.8913	7.48970	9.89
RPLA_3	0.98690	49.1720	5.01939	6.63
RPLA_4	1.17013	61.7957	5.30909	7.01
RPLA_5	0.80979	49.7159	5.01939	6.63
Average	1.02674	54.9871	7.15043	9.442
Standard Deviation	0.20081	5.43779	3.38430	4.46687
Range	0.48060	12.6237	7.89521	10.42

DNIR Board ABS and PLA Readings

Red ABS DNIR Readings

	led1	led2	led3	led4	led5	led6	led7	led8
0	0.328867	0.436332	0.455028	8.30E-05	8.34E-06	0.000151	0.00011	0.115158
1	0.328926	0.436442	0.455149	3.30E-05	0.000156	0.000119	8.34E-06	0.115302
2	0.328873	0.436453	0.455232	8.50E-05	1.50E-05	0.000173	0.000141	0.115205
3	0.328939	0.436375	0.455161	0.000175	8.90E-05	3.58E-06	5.96E-07	0.115302
4	0.328856	0.436505	0.455199	1.80E-05	0.000113	0.000162	5.70E-05	0.11527
5	0.328886	0.436367	0.455291	0.000114	1.50E-05	6.80E-05	0.000129	0.115239
6	0.328904	0.43652	0.455235	5.90E-05	0.000147	7.30E-05	2.30E-05	0.115355
7	0.328776	0.436457	0.455329	8.70E-05	3.00E-05	0.000127	0.000142	0.115243
8	0.328783	0.436524	0.455329	4.20E-05	2.10E-05	0.000143	9.50E-05	0.115256
9	0.328835	0.436416	0.455322	0.000158	6.40E-05	2.20E-05	0.000159	0.115305

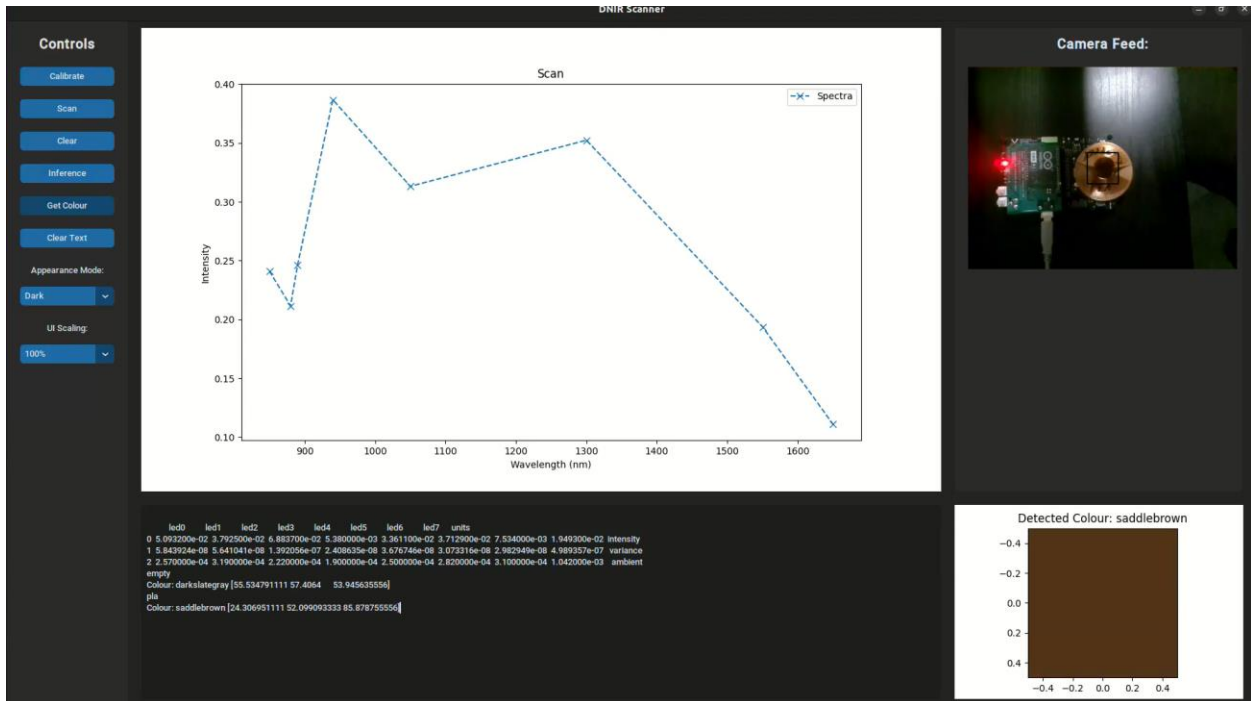
Red PLA DNIR Readings

	led1	led2	led3	led4	led5	led6	led7	led8
0	0.280607	0.363147	0.385984	0.000162	0.000425	0.000475	0.000207	0.117306
1	0.280717	0.362802	0.386094	0.00051	0.000252	0.000291	0.000483	0.117383
2	0.280759	0.362763	0.386016	0.000514	0.000213	0.000206	0.000476	0.117404
3	0.280408	0.36311	0.386068	0.000155	0.000365	0.00049	0.000209	0.117285
4	0.280755	0.363113	0.385895	0.000313	0.000458	0.000325	4.77E-06	0.117568
5	0.280684	0.362738	0.38612	0.000475	0.000238	0.000224	0.000476	0.117389
6	0.280463	0.362889	0.386231	0.000339	0.000146	0.00049	0.000406	0.117225
7	0.280575	0.362766	0.386248	0.000441	0.000152	0.00034	0.000473	0.117342
8	0.280682	0.362896	0.386016	0.000494	0.000321	0.000154	0.000456	0.117543
9	0.280466	0.363121	0.386112	0.000303	0.000464	0.000439	0.000159	0.117435

Product Demonstration: 10-2023-VIDEO Rev. 1

Team 10, 3cycle

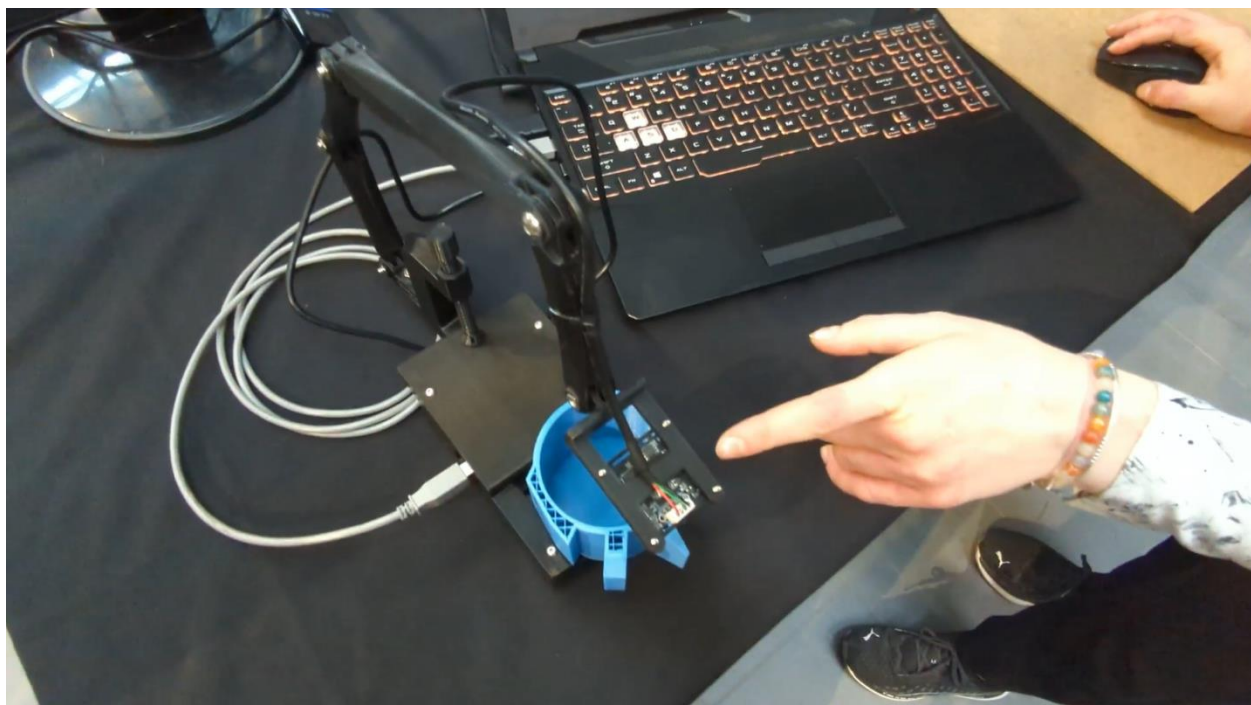
This video can be accessed [on Google Drive](#).



Product Demonstration: 10-2023-VIDEO Rev. 2

Team 10, 3cycle

This video can be accessed [on Google Drive](#).



Appendix C

Design Project Management Data

Schedule: 10-2022-SCHD Rev 4

Team 10, 3cycle

Tasks	Weeks								R1 Sep. Sep. Sep. Oct. Oct. Oct. Nov. Nov.	R2 Oct. Oct. Oct. Nov. Nov.	E1 Nov. Dec.	Holidays Jan 9 Jan 16 Jan 23 Jan 30 Feb 6 Feb 13 Feb 20 Feb 27 Mar 6 Mar 13 Mar 20 Mar 27 Apr 3 Apr 10 Apr 17	DPR3 Feb 30 Mar 6 Mar 13 Mar 20 Mar 27 Apr 3 Apr 10 Apr 17	SYMP Mar 27 Apr 3 Apr 10 Apr 17	DPE2 Apr 17	
	Sep.	Sep.	Sep.	Oct.	Oct.	Oct.	Nov.	Nov.								
Project and Scrum Setup	-	-	-	-	-	-	-	-	-	-	-	-	-	-	-	-
Problem Definition	-	-	-	-	-	-	-	-	-	-	-	-	-	-	-	-
Needs Analysis	-	-	-	-	-	-	-	-	-	-	-	-	-	-	-	-
Market Research	-	-	-	-	-	-	-	-	-	-	-	-	-	-	-	-
Report	-	-	-	-	-	-	-	-	-	-	-	-	-	-	-	-
Poster	-	-	-	-	-	-	-	-	-	-	-	-	-	-	-	-
Environment and Safety Research	-	-	-	-	-	-	-	-	-	-	-	-	-	-	-	-
Waste Sample Acquisition	-	-	-	-	-	-	-	-	-	-	-	-	-	-	-	-
Lab Training	-	-	-	-	-	-	-	-	-	-	-	-	-	-	-	-
Recycle Samples	-	-	-	-	-	-	-	-	-	-	-	-	-	-	-	-
Polymer Distinction Research	-	-	-	-	-	-	-	-	-	-	-	-	-	-	-	-
Decide Contamination Compositions	-	-	-	-	-	-	-	-	-	-	-	-	-	-	-	-
Spectroscopy Baseline Measurements	-	-	-	-	-	-	-	-	-	-	-	-	-	-	-	-
Contain. Sample Chem Properties	-	-	-	-	-	-	-	-	-	-	-	-	-	-	-	-
Contaminated sample differentiation	-	-	-	-	-	-	-	-	-	-	-	-	-	-	-	-
Source Polymer ID C Components	-	-	-	-	-	-	-	-	-	-	-	-	-	-	-	-
Assemble PolyID Board	-	-	-	-	-	-	-	-	-	-	-	-	-	-	-	-
Testing & Verification PolyID Board	-	-	-	-	-	-	-	-	-	-	-	-	-	-	-	-
Firmware Setup & Flash Testing	-	-	-	-	-	-	-	-	-	-	-	-	-	-	-	-
Prototyping & Redesign PolyID Board	-	-	-	-	-	-	-	-	-	-	-	-	-	-	-	-
Source new PolyID board components	-	-	-	-	-	-	-	-	-	-	-	-	-	-	-	-
PolyID v2 Board Manufactured	-	-	-	-	-	-	-	-	-	-	-	-	-	-	-	-
PolyID v2 Testing & Refine	-	-	-	-	-	-	-	-	-	-	-	-	-	-	-	-
Set Up Colour ID with CVision	-	-	-	-	-	-	-	-	-	-	-	-	-	-	-	-
Algorithm Development	-	-	-	-	-	-	-	-	-	-	-	-	-	-	-	-

Budget: 10-2022-BUDG Rev 2

Team 10, 3cycle

Purchases										
Item Name	Status	Purpose	Source	Ship. Time	Merch. Cost (+ HST)	Shipping Cost	Discnt .	Total Cost	Buyer	Invoice
Digikey Order	Avail.	Dev board parts	Digikey	1-3 day	209.95	0	0	-209.95	Urban	Invoice
C6186 Volt. Regulat.	Avail.	Dev board parts	LCSC Electronics	1 wk	0.74	8.57	0	-9.31	Urban	Invoice
WinSource Order	Avail.	Dev board parts	WINSOURCE	<1 wk	292.03	48.3	-15	-325.33	Urban	Invoice
7.68 MHz crystal	Avail.	Dev board parts	Newark	<1 wk	0.68	11.99	0	-12.67	Urban	Invoice
PCB	Avail.	Dev board parts	JLCPCB	<1 wk	12	30.58	-10	-32.58	Urban	Invoice
LM285D -2-5	Avail.	Dev board parts	Texas Instr.	<1 wk	11.84	17	0	-28.84	Urban	Invoice
Prototy. Order	Avail.	Prototy. compnts.	Digikey	1-3 day	36.67	8	0	-44.67	Urban	Invoice
ABS Filament	Avail.	Polymer testing	Amazon	2 day	47.83	0	-1.34	-46.49	Urban	Invoice
ABS Filament	Avail.	Testing samples	Amazon	2 day	17.44	0	0	-17.44	Urban	Invoice
V2.0 order	Avail.	Dev board v2.0 parts	Digikey	1-3 day	416.25	0	0	-416.25	Urban	Invoice
Poster Printing	Avail.	Capstone symposia	Conference Posters	2 day	76.66	0	0	-76.66	Julia	Invoice
Purchases Subtotal								-1,220.19		
Funding										
University of Waterloo Department of Engineering				Department Funding at \$70 per student per term, 4 students, 2 terms				+560	Note: any 3cycle funding not used in this design project will be dedicated to	
				Social Impact Fund				+3,000		

3cycle	Sustainability Action Fund	+1,200	developing other tasks in 3cycle recycling process
	Funding Subtotal:	+4,760	
Labour Hours			
Team 10	4 Students	6 hr/wk	28 wks

\$16/hr* (theoretical)

-10,752

*\$0/hr (real)

Organizational Roles: 10-2022-ROLES Rev 1

Team 10, 3cycle

- Project Management Lead (Julia)
 - Project Management Secondary (Mohamed)
- Chemistry Lead (Mohamed)
 - Chemistry Secondary (Maria)
- Automation Lead (Urban)
 - Automation Secondary (Julia)
- Process Design Lead (Maria)
 - Process Design Secondary (Urban)
- Business Consultant (Jason)

Register of Risks: 10-2022-RISK Rev 3

Team 10, 3cycle

	Risk	Mitigation
Non-Technical Risks	Long delays in shipping	Ordering early, end of January
	Package delivery complications or package theft	Ordering packages to a shipping address which is a house instead of an apartment complex
Technical Risks	Composite materials may cause contamination or equipment damage	Redundancy in sorting: e.g., eddy current, human operator
	Samples with too much empty space (e.g. stringy failed prints) may not be classified correctly	Stringy pieces rejected for now. Recommended to increase sample collection for further ML model training and verification.
	Equipment maintenance	Dedicating contingency time to fix and maintain equipment; adapting procedures to make use of backup equipment

Appendix D

Knowledge Application

Analog to Digital Conversion

Resolution of Voltage to ADC

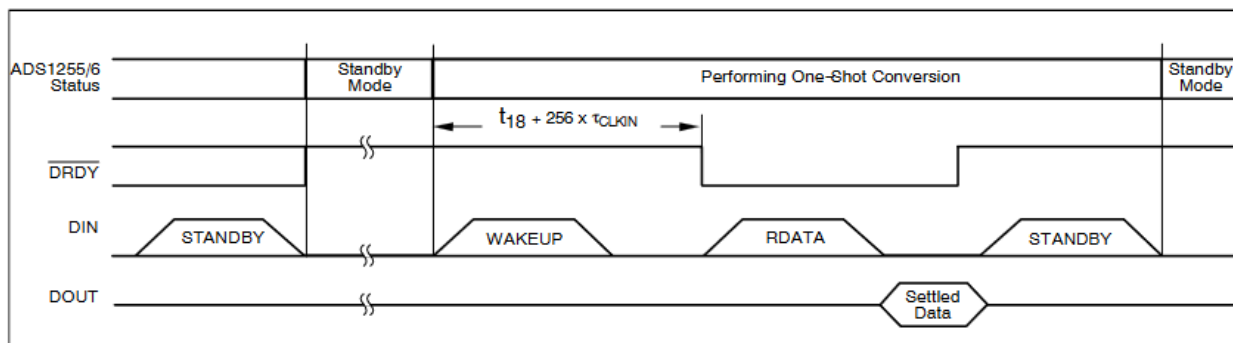
$$\frac{\text{Resolution of the ADC}}{\text{System Voltage}} = \frac{\text{ADC Reading}}{\text{Analog Voltage Measured}}$$

ADC Voltage Resolution

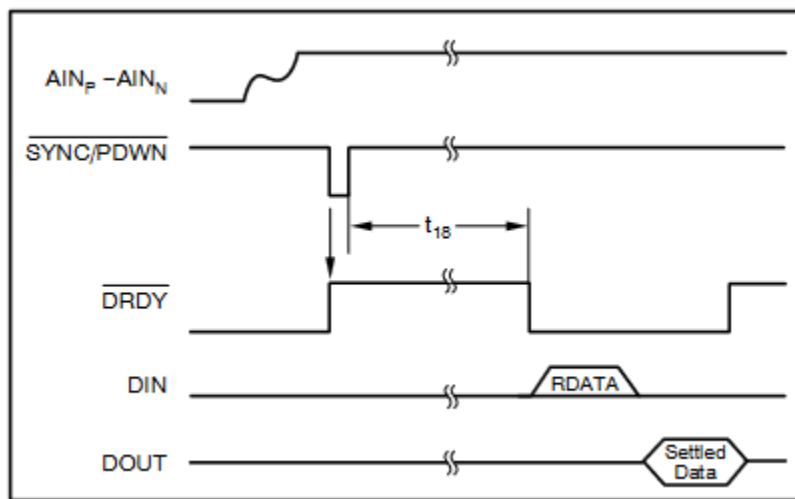
$$Q = \frac{E_{\text{FSR}}}{2^M}$$

ADS1256 Reading Timing Diagrams

One-Shot Conversion

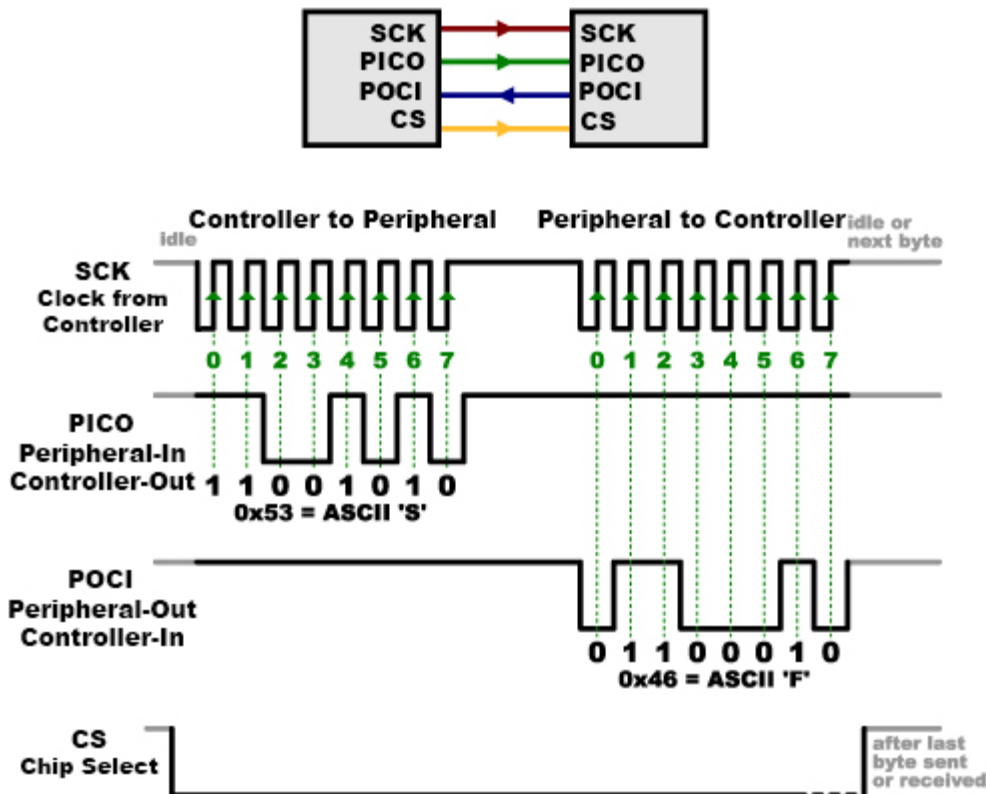


Data Retrieval After Synchronization

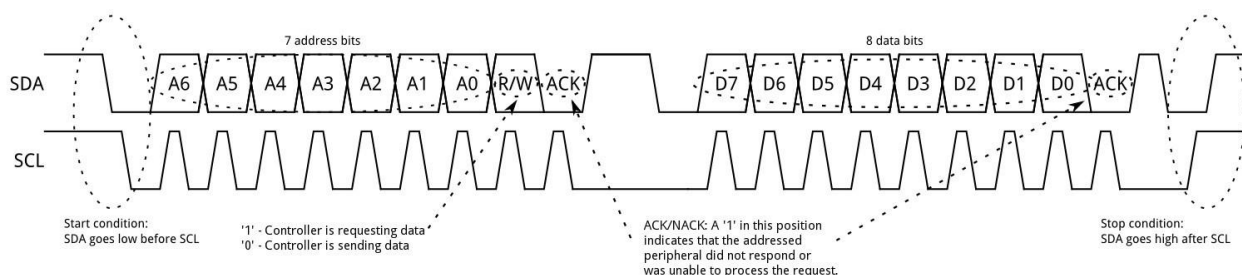


Serial Protocols

SPI Protocol



I2C Protocol



Data Science

Standard Deviation

$$\sigma = \sqrt{\frac{\sum(x_i - \mu)^2}{N}}$$

σ = population standard deviation

N = the size of the population

x_i = each value from the population

μ = the population mean

Min / Max Normalization

$$x_{scaled} = \frac{x - x_{min}}{x_{max} - x_{min}}$$

Boolean Logic

Bitwise AND

p	q	F^0	NOR^1	Xq^2	$\neg p^3$	$\neg\cdot^4$	$\neg q^5$	XOR^6	$NAND^7$	AND^8	$XNOR^9$	q^{10}	$If/then^{11}$	p^{12}	$Then/if^{13}$	OR^{14}	T^{15}
1	1	0	0	0	0	0	0	0	0	1	1	1	1	1	1	1	1
1	0	0	0	0	1	1	1	1	1	0	0	0	1	1	1	1	1
0	1	0	1	1	0	0	0	1	1	1	0	1	1	0	0	1	1
0	0	0	1	0	1	0	1	0	1	0	1	0	1	0	1	0	1
Bitwise equivalents		0	NOT ($p \text{ OR } q$)	($\text{NOT } p$) AND q	NOT p	$p \text{ AND }$ ($\text{NOT } q$)	$p \text{ AND }$ q	$p \text{ XOR } q$	NOT ($p \text{ AND } q$)	$p \text{ AND } q$	NOT ($p \text{ XOR } q$)	q	($\text{NOT } p$) OR q	p	$p \text{ OR }$ ($\text{NOT } q$)	$p \text{ OR } q$	1

Computer Science

UTF-8 Encoding

Code point \leftrightarrow UTF-8 conversion

First code point	Last code point	Byte 1	Byte 2	Byte 3	Byte 4	Code points
U+0000	U+007F	0xxxxxxxx				128
U+0080	U+07FF	110xxxxx	10xxxxxx			1920
U+0800	U+FFFF	1110xxxx	10xxxxxx	10xxxxxx		[nb 2]61440
U+10000	[nb 3]U+10FFFF	11110xxx	10xxxxxx	10xxxxxx	10xxxxxx	1048576

Baud Rate

$$T_s = \frac{1}{f_s}$$

Hardware

Instrumentation Op-Amp Gain

$$A_v = \frac{V_{\text{out}}}{V_2 - V_1} = \left(1 + \frac{2R_1}{R_{\text{gain}}}\right) \frac{R_3}{R_2}$$

Spectroscopy

Discrete Fourier Transform

$$\begin{aligned} X_k &= \sum_{n=0}^{N-1} x_n \cdot e^{-\frac{i2\pi}{N} kn} \\ &= \sum_{n=0}^{N-1} x_n \cdot \left[\cos\left(\frac{2\pi}{N} kn\right) - i \cdot \sin\left(\frac{2\pi}{N} kn\right) \right], \end{aligned}$$

Spectral Directional Transmittance

$$\begin{aligned} T_{\nu,\Omega} &= \frac{L_{e,\Omega,\nu}^t}{L_{e,\Omega,\nu}^i}, \\ T_{\lambda,\Omega} &= \frac{L_{e,\Omega,\lambda}^t}{L_{e,\Omega,\lambda}^i}, \end{aligned}$$

where

- $L_{e,\Omega,\nu}^t$ is the spectral radiance in frequency *transmitted* by that surface;
- $L_{e,\Omega,\nu}^i$ is the spectral radiance received by that surface;
- $L_{e,\Omega,\lambda}^t$ is the spectral radiance in wavelength *transmitted* by that surface;
- $L_{e,\Omega,\lambda}^i$ is the spectral radiance in wavelength received by that surface.